

Hydraulic Properties of Geosynthetic Clay Liners

A Thesis

Presented to the faculty of the School of Engineering
and Applied Science

University of Virginia

in partial fulfillment
of the requirements of the degree

Master of Science

By

Thomas Rocco Williams

May 2018

Abstract

The long-term quality of groundwater resources requires careful waste management. One vulnerability results from the percolation of rainwater through various types of landfills; the resulting leachate may contaminate groundwater. Modern landfill design employs composite lining systems along the base and along the top cover after closure to mitigate potential environmental damage. Multiple layers of different materials, including geosynthetics, work together at the base to collect leachate and to prevent it from leaving the landfill. Geosynthetic clay liners (GCLs) are composite materials which utilize the swelling ability of bentonite clay to slow seepage by restricting the hydraulic conductivity. GCLs are deployed in top and bottom liner systems, and studies of GCLs in laboratory and field conditions show that GCLs may maintain long-term hydraulic conductivities $<10^{-10}$ m/s to a variety of solutions.

The strengths and susceptibilities of GCL products must be considered during the design and installation of liner systems to ensure long-term performance as adequate hydraulic barriers. The goal of the research herein is to promote the understanding of the hydraulic behavior of GCL deployed in the field. The primary study analyzes the effects of an extended atmospheric exposure upon the hydraulic properties of GCL in a composite landfill liner system (geomembrane overlying GCL). Properties of the GCL varied between favorable and severely degraded, depending on location along the slope length. Measured hydraulic conductivities of exhumed GCL ranged between 10^{-11} - 10^{-6} m/s. Evidence of down-slope bentonite erosion was observed at mid-slope and slope-bottom locations.

During the secondary study herein, research was conducted to improve the characterization of polymer content in bentonite-polymer mixtures. These mixtures provide GCLs with increased chemical resistance to certain highly concentrated waste leachates. Accurately and precisely quantifying the distribution of polymer in these mixtures is necessary to achieve reliable and consistent mixture properties for use in bentonite-polymer GCL products.

Acknowledgements

I would like to start by extending my sincere thanks to my advisor, Dr. Craig Benson, for his patience, guidance, and encouragement throughout the research process. My understanding of the role, importance, and responsibility of engineering has fundamentally improved thanks to his mentorship.

I would also like to thank my committee chairs, Dr. James Smith and Dr. Lindsay Ivey-Burden.

I am grateful to Dr. Nazli Yesiller and Dr. James Hanson at the California Polytechnic State University, who oversaw the exhumation of GCL at the primary study site. Their guidance in setting up the experimental design was invaluable to the exposure study herein.

I am also thankful to Dr. Kuo Tian, who provided guidance and mentorship during my graduate studies. His support and patience while teaching me laboratory procedures and his knowledge as an instructor made my research possible.

To Tony Singh, who was always eager, helpful, and patient, I extend my sincere thanks. His vast knowledge of analytical procedures and equipment enabled me to conduct my research.

I also thank the faculty and staff of the CEE engineering department who have supported me throughout my undergraduate and graduate studies.

I would also like to thank my fellow graduate students in the CEE program. I consider myself very fortunate to have worked with and learned from the academically and personally diverse backgrounds and areas of expertise which are present in the CEE program. I believe that I've become a better team member and person thanks to the example set by my colleagues. I am proud to have been a part of the program.

My parents, Jody and Michael Williams, my family, and my friends have my full gratitude for their ceaseless encouragement, support, and love.

Financial support for this study was provided by the US Department of Energy (DOE) under cooperative agreement DE-FC01-06EW07053 entitled the Consortium for Risk Evaluation with Stakeholder Participation III.

Table of Contents

- Abstract..... 1
- Acknowledgements..... 2
- Table of Contents..... 3
- List of Figures 6
- List of Tables 8
- 1 Introduction 9
- 2 Literature Review: Overview of Hydraulic Conductivity Behavior of Geosynthetic Clay Liners in Laboratory Testing and Field Implementation 11
 - 2.1 Abstract..... 11
 - 2.2 Introduction to Geosynthetic Clay Liners: 11
 - 2.2.1 Bentonite Clay and Montmorillonite Structure: 12
 - 2.2.2 Cation Exchange Capacity and Diffuse Double Layer Theory 12
 - 2.2.3 Water Adsorption and Swelling Mechanisms of Bentonite..... 13
 - 2.2.4 Organic and Inorganic Interactions with Clay and GCLs 14
 - 2.3 Hydraulic Conductivity Testing of Na-Bentonite GCLs..... 15
 - 2.3.1 Inorganic Cation Valence and Concentration Effect on GCL Behavior 16
 - 2.3.2 Effect of Inorganic Cation Species on GCL Behavior 18
 - 2.3.3 Influence of pH on GCL Behavior 19
 - 2.3.4 Effective Stress and Hydraulic Gradient Effects on Hydraulic Conductivity 21
 - 2.3.5 Effects of Prehydration in DI Water Upon the Hydraulic Conductivity of GCLs..... 21
 - 2.4 In Service GCL Behavior and Hydraulic Conductivity of Exhumed GCLs from Landfill Final Covers 23
 - 2.4.1 Hydraulic Properties of Exhumed GCLs..... 24
 - 2.4.2 Exhumed GCL Hydraulic Conductivity - Effects of Permeant Solution 28
 - 2.4.3 Preferential Flow Paths 29
 - 2.5 Modified Bentonite and Bentonite-Polymer Composites – Brief Research Overview 30
 - 2.6 Summary of Findings..... 34
 - 2.7 References 35
- 3 Hydraulic Conductivity of Geosynthetic Clay Liner (GCL) Exhumed from a Composite Liner after 12-yr of Atmospheric Exposure..... 36
 - 3.1 Introduction 37
 - 3.2 Background 38
 - 3.2.1 Relevant Laboratory Testing 38
 - 3.2.2 Previous Exhumed GCL Studies..... 39
 - 3.3 Exhumation and Test Methods..... 41
 - 3.3.1 Exhumation of GCL..... 41

3.3.2	Hydraulic Conductivity	42
3.3.3	Swell Index	43
3.3.4	Mass per Area	43
3.3.5	XRD.....	43
3.3.6	Bentonite Exchange Complex	44
3.4	Results and Discussion	44
3.4.1	Exhumed Condition of GCL	44
3.4.2	Hydraulic Conductivity of Exhumed GCL.....	46
3.4.3	Influence of Subgrade Porewater Chemistry.....	48
3.4.4	Desiccation Effects and Preferential Flow	49
3.5	Summary and Conclusions	50
3.6	Acknowledgement	51
3.7	References	51
3.8	Tables and Figures.....	52
4	Observations of Bentonite Erosion in Composite Liner System Exposed to the Atmosphere for 12 Years.....	66
4.1	Abstract.....	66
4.2	Introduction and Background	66
4.3	Exhumation and Testing Methods.....	68
4.3.1	Mass per Unit Area	68
4.3.2	X-Ray Diffraction	68
4.3.3	Swell Index	69
4.4	Observations of Erosion in Exposed Liner and Discussion.....	69
4.5	Summary and Conclusions	71
4.6	REFERENCES.....	71
4.7	Erosion Observation Tables and Figures.....	72
5	Challenges in Assessing the Polymer Loading of Bentonite Polymer Mixtures.....	77
5.1	Abstract.....	77
5.2	Introduction	77
5.3	Background	79
5.4	Materials and Methods.....	80
5.5	Findings and Discussion	82
5.6	Suggestions for Future Research	83
5.7	References	84
5.8	Tables and Figures.....	85
6	Appendix	88
6.1	Composite Liner Exposure: Regulatory Applicability of Findings	88
6.2	Exposed Liner Project – Additional Testing.....	89

6.3 Additional Figures and Tables	91
References	95

List of Figures

Fig. 2.1. A comparison of 40 mM CaCl ₂ to 100 mM KCL shows the greater effects of the divalent solution on hydraulic conductivity, cation exchange, swelling, and water content, from Jo et al. (2004).	17
Fig. 2.2. RMD and ionic strength (M) vs hydraulic conductivity, with free swell values included for reference, from (Kolstad et al. 2004a).	19
Fig. 2.3. Effect of prehydration from (Jo et al. 2004).	22
Fig. 2.4. Meer and Benson (2007) Hydraulic conductivity testing results on exhumed GCLs permeated with 10mM CaCl ₂ . Note the abrupt change in hydraulic conductivity between 80-100% water content (right figure) and note that the hydraulic conductivity can vary greatly at the same level of divalent cation exchange, as shown by the sodium mole fraction (left figure).	26
Fig. 2.5. Arrows point to desiccation cracks caused by drying, from (Meer and Benson 2007).	27
Fig. 2.6. Cross section picture of GCL interior before the addition of the dye, light area is hydrated bentonite, dark area is a bundle of needle-punched fibers along which preferential flow is suspected to occur, from (Benson et al. 2010).	30
Fig. 2.7. Hydraulic conductivity of BPC GCL relative to conventional GCLs permeated with 1 M NaOH (top) and 1 M HNO ₃ (bottom), from Scalia et al. (2014).	32
Fig. 2.8. Polymer elution fractions after long term hydraulic conductivity testing with varying CaCl ₂ permeant solution strength, from Scalia and Benson (2016).	33
Fig. 3.1. Overhead aerial image of landfill site (left), courtesy of Professor Jim Hanson at Cal Poly San Luis Obispo. White lines indicate approximate exhumation locations of the east and southeast corner slopes. Plan view of landfill slope and locations of GCL sample exhumation (right). Drawing is not to scale. Colored squares indicate GCL exhumation positions. Color corresponds to location along slope (top=blue, middle=orange, bottom/toe=gray, anchor=yellow).	54
Fig. 3.2. Overview of hydraulic conductivity behavior during testing of the exhumed GCL.	55
Fig. 3.3. Exhumed GCL with varying gravimetric water content. The initial condition of the exhumed bentonite varies between gel-like, desiccated, and granular.	56
Fig. 3.4. Average properties of exhumed GCL from varying slope positions. The gravimetric water content was measured using the internal contents of the GCL. The monovalent mole fraction refers to the major bound cation composition of the exhumed bentonite.	57
Fig. 3.5. Exhumed GCL gravimetric water content vs. subgrade soil gravimetric water content (a) and the swell index of the exhumed GCL versus the montmorillonite content. ES = east slope.	58
Fig. 3.6. Hydraulic conductivity with average water versus slope location.	59
Fig. 3.7. Hydraulic conductivity of exhumed GCL versus swell index (a) and swell index versus the major bound cation monovalent mole fraction (X_M) of the exhumed bentonite (b).	60
Fig. 3.8. The gravimetric water content of the exhumed GCL immediately following hydraulic conductivity testing with average water versus the swell index.	61
Fig. 3.9. The monovalent mole fraction of major bound cations on the exhumed GCL bentonite versus the exhumed GCL gravimetric water content (a) and hydraulic conductivity versus exhumed gravimetric water content of GCL (b).	62
Fig. 3.10. The monovalent mole fraction of major bound cations on the exhumed GCL bentonite versus the subgrade total soluble cation charge per mass (TCM) (a) and the GCL TCM versus the subgrade TCM (b). GCL with higher K had $K > 10^{-7}$ m/s and GCL with lower K had $K < 4 \times 10^{-11}$ m/s.	63
Fig. 3.11. The GCL total soluble cation charge per mass (TCM) versus the subgrade soil gravimetric water content (a) and the monovalent mole fraction of major bound cations on the exhumed GCL bentonite versus the subgrade soil water content.	64

Fig. 3.12. Cross sections of GCL with hydraulic conductivity $>10^{-7}$ m/s and varying exhumed water contents. Image (d) shows specimen from (c) following permeation with rhodamine dye.65	
Fig. 4.1. Overhead aerial image of landfill site (left), courtesy of Professor Jim Hanson at Cal Poly San Luis Obispo. White lines indicate approximate exhumation locations of the east and southeast corner slopes. Plan view of landfill slope and locations of GCL sample exhumation. Image is not to scale. Colored squares indicate GCL exhumation positions. Color corresponds to location along slope (top=blue, middle=orange, bottom/toe=gray, anchor=yellow).73	73
Fig. 4.2. Mass per area of whole GCL vs. location.74	74
Fig. 4.3. Rivulets of eroded montmorillonite above GCL exhumed from the middle of the southeast corner slope (SE-M erosion rivulet).74	74
Fig. 4.4. Accumulation of bentonite near the toe of the east slope. The accumulated material lies above the GCL and below the GM. Accumulated material was not included in the mass per unit area measurements.75	75
Fig. 4.5. Area of widespread material accumulation near the bottom of the slope, referred to as the "wedge". Material gathered above the GCL and underneath the GM. Image courtesy of Professor Jim Hanson at Cal Poly San Luis Obispo.75	75
Fig. 4.6. Erosion of the internal contents of GCL exhumed from the bottom of the south slope .76	76
Fig. 5.1. Polymer loading measurements for commercial bentonite-polymer mixture from four operators.....86	86
Fig. 5.2. Comparison of the best estimation of polymer loading following LOI testing vs. the polymer loading based on the initial measured masses of bentonite and polymer. The specimens were prepared by measuring out dried polymer and bentonite under atmospheric conditions.....86	86
Fig. 5.3. Increase in mass of oven-dried (110°C) bentonite-polymer mixture as a function of time since removal from the oven. Sample exposed to atmosphere in laboratory, and three replicate tests were conducted.....87	87
Fig. 5.4. Estimation of polymer loading using air-dried specimen preparation method. Known air-dry batch water contents of the bentonite and polymer were used to calculate the actual polymer loading from initial measured masses.....87	87
Fig. A.6.1. Hydraulic conductivity of sample A1 with deionized water versus the cumulative inflow volume.91	91
Fig. A.6.2. Hydraulic conductivity of sample A2 during wet-dry cycling tests with average water versus the cumulative inflow volume.91	91

List of Tables

Table 3.1. Characteristics of exhumed GCL samples.....	52
Table 3.2. Major mineral constituents of subgrade soil samples determined from X-Ray diffraction (n=14). X-Ray diffraction testing was performed by Mineralogy-Inc.	53
Table 3.3. Average subgrade water content and soluble cation properties relative to location along slope	53
Table 4.1. Properties of GCL exhumed from study site.	72
Table 4.2. Properties of additional erosion specimens.	73
Table 5.1. Polymer loading measurements (%) during initial testing.....	85
Table 5.2. Results of LOI testing of the check specimens using the oven-dry preparation method or the air-dry preparation method.	85
Table A.6.1. Exhumed GCL Exchange Complex – Soluble Cations	92
Table A.6.2. Exhumed GCL Exchange Complex – Major bound cation mole fractions.....	93
Table A.6.3. Subgrade Soil – Soluble Cations.....	94

1 Introduction

The use of geosynthetic materials in environmental and geotechnical applications has grown rapidly in recent decades. The design of leak-resistant barrier systems may employ multiple types of geosynthetics, including polymeric geomembranes and geosynthetic clay liners, to achieve low permeability by utilizing the behavior of each material to form a functional composite system. Geosynthetic clay liners (GCLs) were first employed for field use in the late 1980s, and their usage has spread widely since (Koerner 1990). GCLs typically consist of two geotextiles with a thin layer of sodium-bentonite clay between. The geotextiles are made of synthetic fibers, which eliminate the possibility of biodegradation relative to natural products. The geotextile fibers provide tensile strength to the GCL, which assists the stability of the product on slopes. GCLs may be customized to specific applications by altering the selection of the geotextiles, modifying the bentonite clay, and electing to needle punch the geotextiles. Modifications to the bentonite clay most significantly affect hydraulic behavior.

The hydraulic properties of GCLs are dependent on the bentonite clay. Hydraulic conductivity of the bentonite may vary between $\approx 10^{-11}$ m/s in dilute aqueous solutions to $>10^{-6}$ m/s in concentrated electrolyte solutions. The hydration conditions experienced by GCLs installed in the field influence their long-term hydraulic conductivity behavior, and the primary goal of this study is to contribute to field implementation knowledge. Attempts have been made to modify the bentonite to increase its chemical resistance for concentrated waste applications. Currently, the most successful modification appears to be the addition of polymer to the bentonite. The addition of polymer changes the mechanisms controlling GCL hydraulic conductivity, and polymer-bentonite mixtures may reduce the hydraulic conductivity by multiple orders of magnitude in select conditions (Scalia et al. 2014). The use of these polymer-bentonite mixtures is still relatively new, and additional research into their properties will help to improve

field implementation practices. The secondary goal of this study was to improve and standardize the measurement process for polymer content in bentonite polymer mixtures.

Section 2 introduces the material properties and behavior of geosynthetic clay liners (GCLs). The objectives of the review are to introduce the geosynthetic clay liner, introduce the mechanisms underlying its hydraulic properties, review laboratory research concerning key factors affecting the hydraulic conductivity, to introduce research focused on the exhumed properties of GCLs removed from landfill final covers, and to briefly review the research into amended bentonites that include polymer.

Section 3 details the investigation process and findings for a study of exhumed GCL from a composite liner (GM over GCL) exposed to the atmosphere for 12 yr. Work on this project was completed in coordination with a research team from California Polytechnic State University. The California team oversaw the exhumation of the GCL samples analyzed in this study. There are many previous studies of GCL exhumed from field sites, but the majority of these studies exhumed GCL from landfill final covers with overlying soil. The author is unaware of a previous study exhuming GCL from a landfill bottom liner for hydraulic conductivity testing. Section 4 continues the exhumed GCL analysis by considering the consequences of erosion on the integrity of the GCL.

Section 5 reports on challenges encountered during the measurement of polymer loading of polymer-modified GCL products. Difficulties are present in the process due to the strong water vapor affinity of dried polymer and bentonite, heterogeneity of the distribution of polymer in the GCL product, and variance in the selection of specimen area for testing. Establishing a consistent testing procedure will help to ensure adequate product performance in field implementation.

2 Literature Review: Overview of Hydraulic Conductivity Behavior of Geosynthetic Clay Liners in Laboratory Testing and Field Implementation

2.1 Abstract

Laboratory testing of geosynthetic clay liners (GCLs) shows that their ability to function as hydraulic barriers is highly dependent on the permeant solution's cation concentration, the cation valence, and pH. These factors affect the swelling behavior of sodium bentonite, which determines the amount of bound water in the GCL's pore space responsible for reducing the hydraulic conductivity. Understanding the behavior of GCLs in field usage presents a significant challenge due to the complexity of field conditions and the difficulty of exhumation. The field hydration process is particularly important because it may permanently determine the amount of swelling that the bentonite is capable of. The simultaneous occurrence in the field of dehydration of the bentonite along with polyvalent cation exchange appears to drastically alter the effectiveness of GCLs as hydraulic barriers. For usage in extreme conditions, amended bentonites including polymers have been developed which show promising results from laboratory testing. However, additional research is necessary to fully understand their behavioral mechanisms and long-term effectiveness.

2.2 Introduction to Geosynthetic Clay Liners:

Geosynthetic Clay Liners (GCLs) are a thin (~10 mm) manufactured hydraulic barrier consisting of bentonite clay and two sheets of geotextile material. The production process may apply needle stitching, punching, or adhesive bonding in order to bind a thin layer of bentonite (~4-5.0 kg/m²) between the two geotextiles (Petrov and Rowe 1997; Shackelford et al. 2000). The resulting thin GCL sheets are primarily utilized as hydraulic barriers because of their low hydraulic conductivity to water ($k < 10^{-9}$ cm/s) and cost efficiency. A range of commercial bentonites are readily available, with variance in the mineral properties and form of the bentonite, such as

powdered vs. granular bentonite. Additional differences in available commercial GCL products include the properties of the geotextiles (woven vs non-woven) and the binding method between the textiles and the bentonite. However, the hydraulic properties of the GCL are dominated by the bentonite, and so the following discussion will focus on the clay properties which control the GCL's permeability.

2.2.1 Bentonite Clay and Montmorillonite Structure:

Bentonite is a naturally occurring clay with origins in volcanic ash, and it exhibits a great swelling ability in water and high plasticity (Mitchell 1993). Montmorillonite (MMT), a member of the smectite group of phyllosilicate minerals and a significant constituent of bentonite, is mainly responsible for the hydraulic properties of bentonite. MMT consists of extremely thin sheet particles which allow for an extremely high surface area relative to volume. The structure of MMT is characterized as a 2:1 layer silicate made of sheets held weakly together by van der Waals forces (Morris and Zbik 2009). Each sheet consists of a central aluminum octahedron layer bonded between two adjacent silicon tetrahedron layers. The swelling behavior of MMT results from isomorphous substitution in this basic structure. Aluminum may be replaced by lower valence cations, and aluminum may replace the silicon in the tetrahedron layers. These substitutions result in a net negative surface charge of approximately -0.66 per unit cell (Mitchell 1993). As a result, the interlayer volume of MMT in solution contains exchangeable cations that balance the negative surface charge of the particles.

2.2.2 Cation Exchange Capacity and Diffuse Double Layer Theory

The cation exchange capacity (CEC) of a soil refers to the amount of cations held by the soil that may be exchanged for other cations in solution. The values for CEC are typically given in milliequivalents of hydrogen per 100 g of soil. For montmorillonite, typical CEC values range between 80 to 150 meq/100 g (Mitchell 1993). In addition to isomorphous substitution, broken bonds and replacement of hydrogens in hydroxyl groups may contribute to the clay's demand for

cations. Cation replaceability is mainly determined by valence, and the typical series of cation preference is given by:



The bentonite in GCLs tends to undergo cation exchange in accordance with the above series when more favorable cations are available in the pore water. Quantitatively describing the distribution of these ions in a clay-water system presents a difficult challenge, and researchers have developed several theories. The diffuse double layer theory applies electrostatics to describe the distribution of cations and anions adjacent to negatively charged surfaces. Although the accuracy of the theory is limited to low concentration smectite solutions, it still serves as a useful tool for understanding clay behavior (Mitchell 1993). The theory gives Eq. 1 for the thickness of the layer of ions held by the charged particle surface, termed the diffuse double layer:

$$\frac{1}{K} = \left(\frac{\epsilon_0 D k T}{2 n_0 e^2 v^2} \right)^{\frac{1}{2}} \quad 2.1$$

The value of $1/K$ in Eq. 1 may be understood as the double layer thickness, and ϵ_0 , D , k , and e are constants. Cation valence is represented by v , electrolyte concentration is given by n_0 , and T represents temperature. The equation indicates the acute influence of cation valence upon the double layer thickness. In general, the hydraulic conductivity of MMT tends to be inversely proportional to the double layer thickness.

2.2.3 Water Adsorption and Swelling Mechanisms of Bentonite

Several mechanisms may best explain the process of water adsorption to clay surfaces within an ion field. Hydrogen bonding, ion hydration, attraction by osmosis, and dipole attraction have been considered as potential adsorption processes (Mitchell 1993). Additional research is necessary to understand the exact adsorption and swelling mechanism affecting clays. It is known that swelling occurs during hydration as adjacent clay particles move apart until equilibrium

conditions are achieved (Luckham and Rossi 1999). The cations in the interlayer region determine the extent of particle separation, resulting in two different swelling conditions. The first condition, crystalline swelling, occurs during separation of the clay particles to distances of 10-20 Å as water molecules adsorb in layers to the particle surface and hydrate the interlayer cations. At low concentrations of monovalent cations, the second swelling condition can abruptly increase interlayer separation to 30-40 Å, and possibly as high as several hundred Å, as the repulsive osmotic force causes separation of the montmorillonite layers (Morris and Zbik 2009; Rao et al. 2013). Thus, the osmotic swelling condition can lead to high water contents (over 200%) observed in MMT hydration behavior.

2.2.4 Organic and Inorganic Interactions with Clay and GCLs

Research into clay-organic interactions has grown over the last several decades as engineers and scientists seek improved waste cleanup methods (Mitchell 1993). Organic compounds can interact with clays through processes including adsorption, ion exchange, and intercalation. The critical organic properties affecting clay-organic interaction include polarity, solubility, size, shape, and polarizability (Mitchell 1993). The small pore spaces in clay are not conducive to the transport of large organic molecules. In general, there is only limited interaction between the clay in GCLs and the organics encountered in landfill leachate.

Overall, research indicates that small concentrations of liquid organics, in general, do not seem to adversely affect the hydraulic conductivity of GCLs, whereas concentrated inorganic solutions containing multivalent cations may drastically increase the hydraulic conductivity of sodium bentonite GCLs (Ruhl and Daniel 1997). Previous research indicates that other components of a composite barrier system, such as soil barriers, may be more effective than GCLs in preventing the mass transport of some organic compounds, including Volatile Organic Compounds (VOCs) (Eun et al. 2017; Foose et al. 1999). Certain contaminants, such as benzene and toluene, may be sorbed to geotextile (Rowe et al. 2005). Some research has been attempted

to improve the resistance of GCLs to certain organic pollutants. Researchers considered combinations of bentonite with organoclays and activated carbon to increase VOC sorption to GCLs, but contaminant transport modeling found only slight changes in VOC transport (Lake and Rowe 2005). Organic pollutant interactions with GCLs remain an important research area in need of additional investigation. This review will instead focus on the wealth of research surrounding the behavior of GCLs permeated with inorganic solutions. Inorganic cation interactions remain critically important because of the natural prevalence of divalent cations in soils and their ability to dramatically affect the hydraulic conductivity of GCLs.

2.3 Hydraulic Conductivity Testing of Na-Bentonite GCLs

The following research pertains to Na-Bentonite GCLs tested in flexible wall permeameter cells with a variety of permeant solutions. A study by Petrov et al. (1997) found that hydraulic conductivity values were comparable across multiple permeameter types for a given stress level and permeant solution. However, rigid-wall permeameters may experience issues with sidewall leakage where gaps exist between the GCL sample and the rigid holding wall. By using a permeameter with a flexible membrane wall, good contact between the GCL sample and membrane is more easily achieved (Shackelford et al. 2000). Termination criteria may vary between tests, but general conditions include the near equality of inflow and outflow rates, measurement of steady hydraulic conductivity values, and the similarity of the chemical composition of the effluent and influent. When chemical composition analysis is prohibitive due to time and expense, measurements of electrical conductivity and pH may be used as composition indices. Deciding when to terminate testing is critical because GCLs frequently experience long term changes in hydraulic conductivity which may require years and hundreds of pore volumes of flow to observe (Jo et al. 2005). Prehydration conditions and confining stress are additional significant testing variables which will be discussed in later sections. Due to the multitude of

testing variables, the hydraulic conductivity values in the following data should be interpreted relative to each other rather than as absolutes.

2.3.1 Inorganic Cation Valence and Concentration Effect on GCL Behavior

A significant amount of research demonstrates that increasing either the cation valence or the cation concentration of permeant solutions results in higher long-term hydraulic conductivities of GCLs (Jo et al. 2001, 2004, 2005; Kolstad et al. 2004a; Ruhl and Daniel 1997). Solutions of 100 mM KCl, 20 mM CaCl₂, and 40 mM CaCl₂ were used as permeant in Jo et al. (2004). The tests were conducted using the falling-head method with constant tailwater and no backpressure, and four to six replicate tests were conducted for each treatment category. Results found that even though K⁺ mostly replaced CaCl₂ in the bentonite exchange complex, the 100 mM KCl solution did not significantly alter hydraulic conductivity nor water content of the GCLs. The hydraulic conductivity remained comparable to that obtained with deionized water (<10⁻⁸ cm/s). The CaCl₂ solutions both resulted in long term (about one year after the test start, or 100 pore volumes of flow) hydraulic conductivities greater than the GCL permeated with the 100 mM KCl solution, as shown by Fig. 2.1 below.

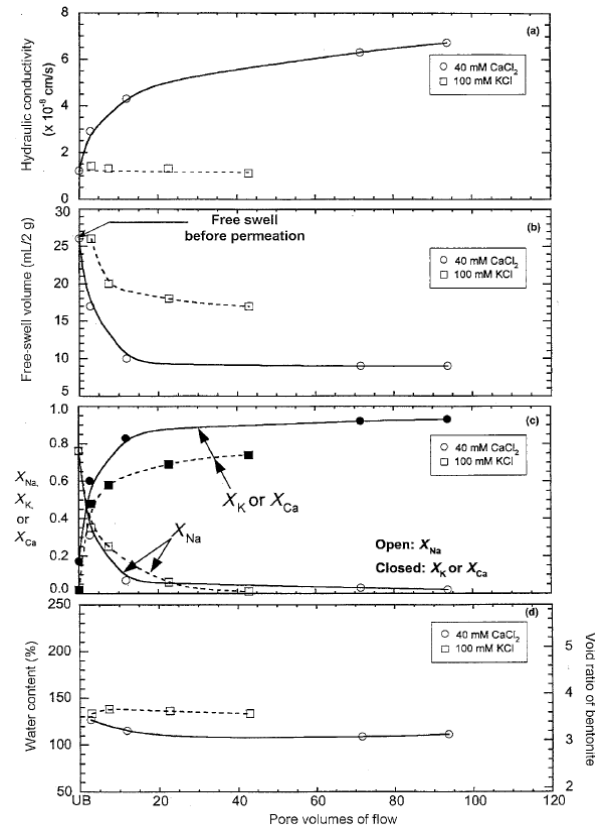


Fig. 2.1. A comparison of 40 mM CaCl₂ to 100 mM KCl shows the greater effects of the divalent solution on hydraulic conductivity, cation exchange, swelling, and water content, from Jo et al. (2004).

The increase in CaCl₂ permeant concentration from 20 mM to 40 mM correlated with a smaller water content, more rapid increase in hydraulic conductivity, and greater long-term value of hydraulic conductivity by a factor of about 3 in the more concentrated specimen. A subsequent study by Jo et al. (2005) used a longer test period and confirmed the previous results. Weak divalent solutions were shown to gradually increase GCL hydraulic conductivity by a factor of 3-15 relative to DI water permeant, and strong divalent solutions (CaCl₂ \geq 50 mM) resulted in an increase of about 3 orders of magnitude (to 1.0×10^{-6} cm/s) relative to DI water. With the strong divalent solution, equilibrium hydraulic conductivity was quickly achieved. The research also varied the initial hydration state of the GCLs which will be discussed in a subsequent section.

2.3.2 Effect of Inorganic Cation Species on GCL Behavior

A study by (Jo et al. 2001) considered the effect of cation species, valence, pH, and concentration on swelling and hydraulic conductivity of non-prehydrated GCLs. Swell testing with the monovalent cations Na^+ , K^+ , and Li^+ showed that larger hydrated ionic radii correlated with larger swelling. The larger swell values were due to the larger cations occupying a greater volume in the interlayer during osmotic swelling. The same study considered the influence of divalent and trivalent species, and it found that swell volumes varied significantly with valence, with the multivalent solutions exhibiting much less swelling. It is believed that the hydrated radius does not significantly affect the swell volume of the multivalent species because of the lack of osmotic swelling. Hydraulic conductivity testing found the free swell trends to be applicable; a reduction in the size of the hydrated monovalent cation correlated with an increase in hydraulic conductivity. Generally, the hydraulic conductivity of different monovalent cation species at the same concentration remained within about one order of magnitude. No hydraulic conductivity trend was noticeable with varying the species of divalent and trivalent cations. The effect on hydraulic conductivity of increasing valence or increasing concentration were much more significant than the identity of the cation species. A change in cation valence at moderate concentration could cause a multiple order of magnitude increase in hydraulic conductivity values, with the effect most noticeable during a change from monovalent to divalent cations at 0.1 M (from 10^{-9} to 10^{-4} cm/s). An increase in the concentration of the monovalent solutions from 0.1 M to 1 M also resulted in a several orders of magnitude increase in hydraulic conductivity.

The effect of solutions containing a combination of cation species was considered by (Kolstad et al. 2004a). Swell and hydraulic conductivity testing was conducted on solution combinations containing Li-Ca, Na-Mg, and Li-Na-Ca-Mg cations. An RMD parameter was defined as the ratio of the concentrations of monovalent to divalent cations in the permeant solution (Eq. 2.2).

$$RMD = \frac{M_M}{\sqrt{M_D}} \quad 2.2$$

In Eq. 2.2, M_M is the total molarity of monovalent cations and M_D is the total molarity of divalent cations. The results found that hydraulic conductivity and swelling behaved independently of the specific cation species in solution, but rather depended on the solution's ionic strength and RMD, as shown in Fig. 2.2.

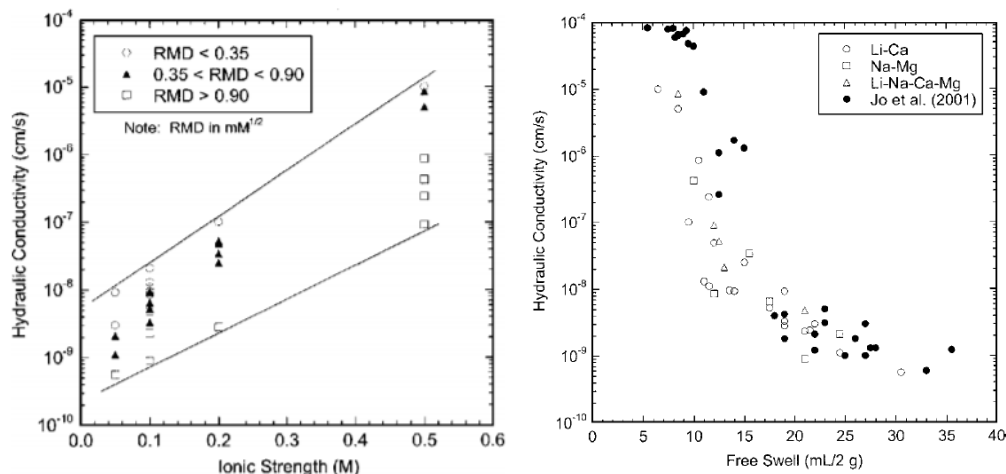


Fig. 2.2. RMD and ionic strength (M) vs hydraulic conductivity, with free swell values included for reference, from (Kolstad et al. 2004a).

The ionic strength appeared directly proportional to the hydraulic conductivity and inversely proportional to swell, whereas the RMD parameter appeared inversely proportional to hydraulic conductivity and directly related to the swell. In weaker solutions with low ionic strength (~ 0.05 M), RMD mainly influenced the hydraulic conductivity and swelling. Concentration controlled at high ionic strengths (~ 0.5 M).

2.3.3 Influence of pH on GCL Behavior

Hydraulic conductivity tests with varying permeant pH have found increased hydraulic conductivity values at extremely basic and acidic pH conditions (Jo et al. 2001; Ruhl and Daniel 1997). Jo et al. (2001) found sharply reduced swelling of sodium bentonite at pH values below 2

and above 12. The extreme pH swell values dropped to about 20 mL, compared with an average of about 35 mL in between the extremes. The hydraulic conductivity trend followed the inverse of the swell values, but the overall trend with pH was less pronounced for hydraulic conductivity. The hydraulic conductivity of GCLs permeated with strongly acidic solutions prepared with DI water (no added divalent cations) experienced very high hydraulic conductivities ($> 10^{-5}$ cm/s) compared with GCLs permeated with more neutral solutions ($\sim 10^{-9}$ cm/s). When the GCLs were permeated with dilute calcium solutions (10 mM and 25 mM) of varying pH, the presence of the divalent cations appeared to partially mask the effect of pH. The acidic calcium solutions (pH = 2) still experienced a significant increase in hydraulic conductivity relative to the other pH values, especially for the 10mM solution (from $\sim 10^{-9}$ to 5×10^{-7} cm/s). No increase in hydraulic conductivity was observed for the calcium solutions at pH = 12 relative to the more neutral pH values. Ruhl and Daniel (1997), permeation of a GCL with a strong base solution (pH = 13) of NaOH produced a large hydraulic conductivity value.

Jo et al. (2001) observed the dissolution of clay particles in strongly acidic solution but not in strongly basic solution, which may explain the mechanisms affecting hydraulic conductivity. Hydrolysis in acidic solution can cause the alumina in the octahedral layers of montmorillonite to dissolve. The researchers analyzed the effluent composition from the hydraulic conductivity testing and found Al in the strong acid effluent but not in the neutral nor basic effluent. In the acidic solution, exchange of Al^{3+} for Na^+ would have occurred, decreasing the amount of bound water in the pore space. Thus, it appears that dissolution of the clay led to the high hydraulic conductivities at the low pH values. Jo et al. (2001) and Ruhl and Daniel (1997) agree that dissolution of clay particles does not explain the hydraulic conductivity of high pH permeant solutions. Instead, the increase in hydraulic conductivity was attributed to the high electrolyte concentration in the strong base solution from the Na^+ cations.

2.3.4 Effective Stress and Hydraulic Gradient Effects on Hydraulic Conductivity

Laboratory testing indicates that increasing the effective stress acting on the GCL decreases the hydraulic conductivity, but the effect is usually limited to within an order of magnitude (Jo et al. 2001; Petrov et al. 1997a; b). Jo et al. (2001) varied effective stresses between 20-500 kPa and found the hydraulic conductivity to vary by less than a factor of 10. Shackelford et al. (2000) varied effective stress from 14 to 140 kPa and found the hydraulic conductivity to decrease by about one-half of an order of magnitude. As the effective stress increases, the tortuosity of the pore space increases, reducing the hydraulic conductivity. Multiple studies showed hydraulic gradient to have a relatively small effect on hydraulic conductivity testing of GCLs provided that the average effective stress is kept constant (Jo et al. 2001; Petrov et al. 1997a; b). The lack of influence of the hydraulic gradient is attributed to the relatively small thickness of GCLs (usually 5 to 15 mm), which causes the effective stress to only vary slightly with large hydraulic gradients. As a result, it is common to run hydraulic conductivity tests with GCLs with much larger hydraulic gradients than for large soil samples (Jo et al. 2004; Kolstad et al. 2004a; Shackelford et al. 2000).

2.3.5 Effects of Prehydration in DI Water Upon the Hydraulic Conductivity of GCLs

Jo et al. (2004) examined the prehydration effect for a GCL permeated with 40 mM CaCl_2 by hydrating the GCL in deionized (DI) water prior to the start of hydraulic conductivity testing. The prehydrated GCL maintained a lower hydraulic conductivity value in the long term by a factor of about 3. Additionally, the prehydrated GCL reached equilibrium at a faster rate than the non-prehydrated sample after permeation with CaCl_2 started (~10 PVF vs ~100 PVF), as shown in Fig. 2.3.

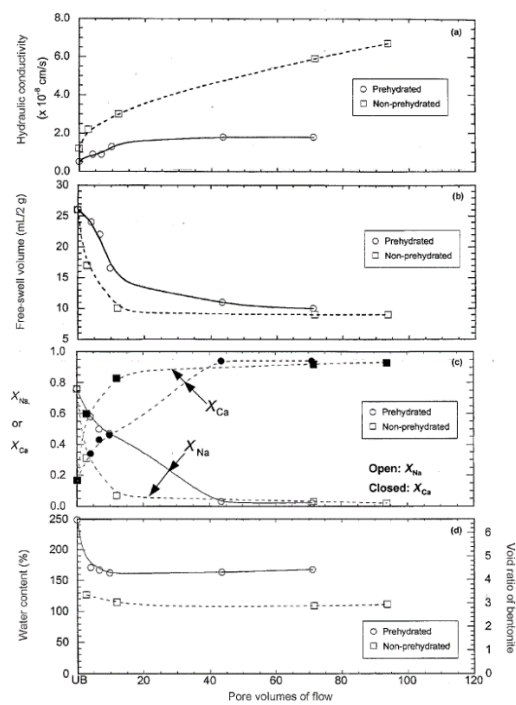


Fig. 2.3. Effect of prehydration from (Jo et al. 2004).

It was hypothesized that the lower hydraulic conductivity resulted from greater retention of immobile water in the prehydrated GCL. Since the initial permeant solution for both samples was dilute, hydration was able to occur in both GCLs before the gradual exchange of Ca^{2+} for Na^{+} was complete. The authors believed that prehydration may result in a different swelling state than direct permeation of a dry bentonite with a concentrated solution. Vasko et al. (2001) examined the effect of partial prehydration on hydraulic conductivity by using a wide range of CaCl_2 solution concentrations as permeant upon GCLs of varying prehydration states. Results showed a two order of magnitude reduction in hydraulic conductivity for a strong (1000 mM) monovalent permeant solution as the initial water content increased from 9% to 200%. The prehydration influence appeared to weaken for permeant concentrations below 100 mM, and initial water contents greater than 200% did not cause additional decreases in hydraulic conductivity.

Lee and Shackelford (2005) and Petrov and Rowe (1997) both observed a permeant concentration dependency for the effect of prehydration with distilled water upon the hydraulic conductivity of GCLs. Petrov and Rowe (1997) prehydrated some GCLs in distilled water and

others in salt water and observed that at high permeant NaCl concentrations (> 600 mM), the GCLs prehydrated in salt water experienced hydraulic conductivities up to two orders of magnitude greater than the GCLs prehydrated in distilled water. At low NaCl concentration (< 100 mM), the effect of prehydration appeared minimal. Lee and Shackelford (2005) showed a concentration dependency by varying the concentration of CaCl₂ permeant solutions and the GCLs' state of hydration. For CaCl₂ solutions between 5 to 50 mM, the effect of prehydration with DI water appeared negligible. However, at a concentration of 100 mM, the effect appeared significant as the non-prehydrated GCL reached a hydraulic conductivity at chemical equilibrium 3 times greater than the prehydrated sample.

Despite the previous findings, it should not be assumed that a GCL prehydrated in dilute solution will maintain low hydraulic conductivity to relatively strong electrolyte solutions. Shackelford et al. (2010) found that GCLs prehydrated in groundwater were susceptible to large increases in hydraulic conductivity when permeated with solutions simulating leachate from mine tailings. The groundwater averaged a pH of 7.2, conductance of 336 μ S, 150 mg/L alkalinity as CaCO₃, and 37 mg/L calcium. The GCL maintained $k \approx 2 \times 10^{-9}$ cm/s to the GW solution. Both mine tailing leachates contained 300-600 mg/L calcium in addition to other metals. Permeation with the main tailing leachates resulted in hydraulic conductivities 2.3-3.9 orders of magnitude larger than those for the GW solution. The prehydration effect was only modest and did not preclude large increases in hydraulic conductivity. Thus, it is very important to conduct testing with site specific leachates to determine whether a given GCL is suitable.

2.4 In Service GCL Behavior and Hydraulic Conductivity of Exhumed GCLs from Landfill Final Covers

The hydraulic conductivity experienced by GCLs installed in the field may vary over several orders of magnitude depending upon a range of conditions including initial and long term changes in hydration state, surrounding soil characteristics, adjacent hydraulic barrier materials,

cation exchange within the GCL, and the formation of preferential flow paths (Benson et al. 2007, 2010; Meer and Benson 2007; Scalia and Benson 2010a, 2011). Measuring the hydraulic conductivity of in-service field GCLs requires excavating the GCL from its liner, a process known as exhumation. The exhumed GCL samples may then be tested using conventional laboratory hydraulic conductivity testing, but careful attention needs to be given to test conditions such as the permeant solution to best replicate field conditions. Lysimeters have also been used to better understand field behavior. The chemistry of the moisture source during initial hydration is important, and the presence of an overlying geomembrane restricts the moisture source to the subgrade soil (Bradshaw et al. 2013; Meer and Benson 2007; Scalia and Benson 2011). A significant portion of in-field GCL behavior may be described as a race between initial hydration and multivalent cation exchange. If an installed GCL can hydrate sufficiently before multivalent cation exchange prohibits osmotic swelling, and if hydration can be continuously maintained, then the hydraulic properties of the GCL are more likely to remain favorable for its purpose as a hydraulic barrier. The following sections will consider existing research into exhumed GCL behavior and testing, starting with the process of hydration and cation exchange.

2.4.1 Hydraulic Properties of Exhumed GCLs

The low hydraulic conductivity of sodium bentonite GCLs is susceptible to drastic increase by a combination of cation exchange and dehydration processes which may occur in the field (Meer and Benson 2007; Scalia and Benson 2010b, 2011). If a geomembrane (GM) is installed directly above the GCL, the interaction between the overlying soil and GCL will be precluded except for GM puncture locations (Rowe 2012). However, advective transport and diffusion from the subgrade soil pore water will still cause exchange with multivalent cations. Porewater of soils adjacent to installed GCLs commonly contain significant amounts of divalent Ca and Mg cations (Mitchell 1993; Scalia and Benson 2011). Existing research indicates that multivalent cation exchange is virtually inevitable for GCLs installed in the field in the long-term. Despite this long-

term trend, the hydraulic conductivity of exhumed GCLs may remain low if osmotic swelling occurs before divalent exchange is complete. Initial osmotic swelling is more favorable when the soil subgrade contains sufficient water content ($>$ optimum) for the GCL to experience rapid hydration (Scalia and Benson 2011). If dehydration is avoided, a GCL that has undergone osmotic swelling can maintain a low hydraulic conductivity and serve its purpose as a hydraulic barrier despite the continued occurrence of divalent cation exchange. However, the occurrence of natural wet and dry cycles may lead to dehydration. When dehydration occurs following divalent cation exchange, research shows that a large increase in the hydraulic conductivity is likely. The following experimental data elaborates on the importance of water content and hydration.

Experimental testing shows an inverse relationship between the exhumed water content of GCLs from final landfill covers and the hydraulic conductivity. Scalia and Benson (2011) examined GCLs exhumed from landfill final covers with overlying geomembranes (GM) that had been in service for 4.7 to 6.7 years. When exhumed GCLs with preferential flow paths are excluded, hydraulic conductivity testing results showed that GCLs with water contents $>$ 53% maintained low hydraulic conductivity ($<$ 5×10^{-9} cm/s) when permeated with 0.01M CaCl_2 . In contrast, GCLs with water contents below $<$ 46% experienced high hydraulic conductivities with 0.01M CaCl_2 permeant, with values as high as 2.1×10^{-5} cm/s. These results were obtained even though substantial exchange of multivalent cations for the original sodium cations had occurred in all GCLs (between 26% of Na exchanged to 99% exchanged). Additionally, a direct correlation was found between the moisture content of the subgrade soil and the exhumed GCL moisture content. Meer and Benson (2007) also tested GCLs exhumed from landfill covers with and without overlying GM, and they found that the hydraulic conductivity changed abruptly for water contents between 80-100%.; their results are shown in Fig. 2.4.

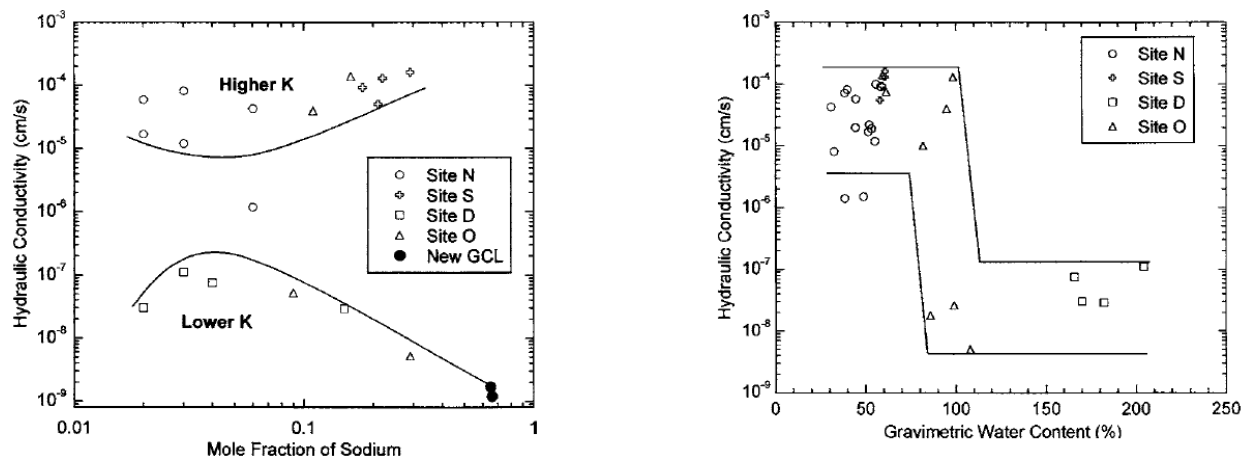


Fig. 2.4. Meer and Benson (2007) Hydraulic conductivity testing results on exhumed GCLs permeated with 10mM CaCl₂. Note the abrupt change in hydraulic conductivity between 80-100% water content (right figure) and note that the hydraulic conductivity can vary greatly at the same level of divalent cation exchange, as shown by the sodium mole fraction (left figure).

Site S had an overlying GM and the most consistent water contents (57.9-60.9%). The other sites, lacking overlying GM, were exhumed with larger ranges in water contents. Below 85% water content, GCLs had high hydraulic conductivities (10⁻⁶ to 10⁻⁴ cm/s), whereas GCLs above 100% water content had lower hydraulic conductivities (10⁻⁸ to 10⁻⁷ cm/s). These values were observed despite extensive divalent cation exchange (> 50%) in all exhumed GCL samples. Site S with overlying GM had the lowest average hydraulic conductivity (<10⁻⁷ cm/s). Following the termination of hydraulic conductivity testing, exhumed GCLs with high hydraulic conductivities retained the least amount of water. For comparison, new GCLs were also tested, and they maintained the lowest hydraulic conductivity values with water contents greater than 200% after testing. Dehydration following divalent cation exchange appears to explain these testing results.

To investigate the dehydration effect upon GCLs, Meer and Benson (2007) took the exhumed GCLs with low hydraulic conductivities and dried them to water contents between 58 and 90% or between 105 and 115%. The samples were then re-permeated. Results found that the controlled desiccation process increased the hydraulic conductivity in all cases. Drying to above 100% water content increased the hydraulic conductivity by 1-2 orders of magnitude, whereas

drying to the lower water contents resulted in a 3-4 order of magnitude increase. Mechanistically, it is believed that dehydration removes the bound water molecules from the interlayer region, including any water from previous osmotic swelling that may have occurred before divalent cation exchange. The removal of bound water reduces the tortuosity of the pore space, possibly allowing advection to control the permeation process rather than diffusion. When advection controls permeation, the resulting hydraulic conductivities may be very high. Additionally, dehydration appears to cause the formation of desiccation cracks in the bentonite, which act as preferred flow channels Fig. 2.5.

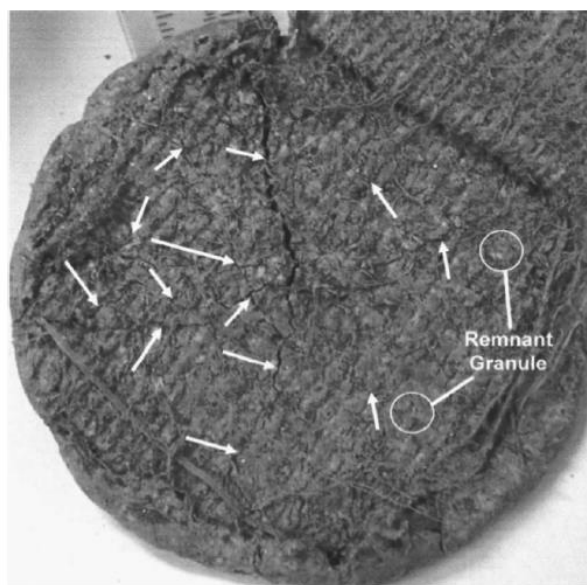


Fig. 2.5. Arrows point to desiccation cracks caused by drying, from (Meer and Benson 2007).

Because of the poor swelling of Ca and Mg bentonite, these cracks are unable to heal upon re-permeating after the occurrence of divalent cation exchange. The dehydration effects become permanent, and the GCL is no longer capable of achieving the intent of its design. As a result of the previous investigations, it is recommended that designers take steps to protect GCLs against simultaneous divalent cation exchange and dehydration. More research is needed to determine

ways in which installed GCLs can be rapidly hydrated and protected from dehydration (Meer and Benson 2007).

2.4.2 Exhumed GCL Hydraulic Conductivity - Effects of Permeant Solution

Scalia and Benson (2010a) found the hydraulic conductivity of exhumed GCLs with low water contents to be highly sensitive to changes in the composition of dilute permeant solutions. Three dilute solutions were tested: type II deionized water (DW), 0.01 M CaCl_2 (Standard Water or SW), and a solution with average characteristics of the eluent from cover soils adjacent to the GCLs (Average Water or AW). The exhumed GCLs with higher water contents ($> 53\%$) maintained similarly low hydraulic conductivities ($< 5 \times 10^{-9}$ cm/s) with all the permeant solutions, except for GCLs containing preferential flow paths. These low hydraulic conductivities were maintained despite the GCLs having extensive divalent cation exchange at the start of testing. The GCLs with lower water contents ($< 46\%$) and no preferential flow paths exhibited much higher hydraulic conductivities with SW permeant ($> 1 \times 10^{-7}$ cm/s) than with AW or DW permeant ($< 2 \times 10^{-9}$ cm/s). The GCLs with lower water contents had undergone less cation exchange at the time of exhumation (likely due to increased diffusion at greater water saturation), indicating that favorable hydration was still possible when permeation occurred with AW or DW. Exchangeable cation measurements of these low water content GCLs showed that AW and DW did not greatly affect the bound cation composition.

Mechanistically, it is believed that the higher water content GCLs had already undergone and maintained osmotic swelling, resulting in low hydraulic conductivities for each of the permeant solutions. The lower water content GCLs, because of the limited amount of divalent cation exchange at the start of testing, could still undergo osmotic swelling if the permeant solution contained favorably low amounts of divalent cations (DW and AW). To best recreate field conditions, it is thus necessary to match the permeant solution as closely as possible to the actual field conditions. Specifically, the subgrade porewater below the GCLs should be considered in

the case of a composite liner with GM overlying GCL, and a permeant solution should be used with matching ionic strength and RMD. If the field conditions are not well known, Scalia and Benson (2010a) suggest that “conservative water” (CW) permeant may be used with 15.5 mg of NaCl (~0.3 mM) and 214.6 mg of CaCl₂ (~2 mM) into 1 L of DW to produce conservative testing results. The hydraulic behavior of GCLs displaying preferential flow paths may be understood by considering an alternative mechanism.

2.4.3 Preferential Flow Paths

In addition to desiccation cracking, preferential flow paths causing large increases in hydraulic conductivity may form in GCLs by other mechanisms. Benson et al. (2010) recorded large hydraulic conductivities ($> 10^{-6}$ cm/s) for multiple exhumed GCL samples from a landfill final cover after about 5 years of service. Nearly total exchange of sodium for calcium had occurred in the exhumed GCLs, but because the GCLs were covered by a geomembrane, the researchers postulated that dehydration had not occurred. Therefore, an alternative explanation was sought for the high hydraulic conductivities besides combined divalent cation exchange and dehydration. Suspecting possible preferential flow paths, a dye was added to the permeant for the testing of exhumed GCLs with high hydraulic conductivities. Upon inspecting the interior of the GCL specimens, the researchers noticed that dark vertical stains followed the bundles of needle-punched fibers (Fig. 2.6). The dye coincided with the fibers, indicating the presence of a preferential flow path. The researchers determined the stains to be manganese oxide, but the mechanism of formation is not currently known, presenting a potential future research opportunity. Scalia and Benson (2010b, 2011) also observed that GCLs with preferential flow paths occurring along bundles of needle-punched fibers acted as exceptions to the general trend of dehydration behavior. The authors hypothesized that cation exchange as water from the subgrade is drawn upwards through the fibers may be the cause. The bentonite adjacent to these fibers did not appear to exhibit osmotic swell.



Fig. 2.6. Cross section picture of GCL interior before the addition of the dye, light area is hydrated bentonite, dark area is a bundle of needle-punched fibers along which preferential flow is suspected to occur, from (Benson et al. 2010).

2.5 Modified Bentonite and Bentonite-Polymer Composites – Brief Research Overview

The desire to improve the performance of GCLs used in extreme conditions has led to several alterations of Na-bentonite. Kolstad et al. (2004b) investigated the hydraulic conductivity of a dense prehydrated (DPH) GCL that is moistened and calendered by the manufacturer. A dilute solution containing sodium carboxymethyl cellulose (Na-CMC) and methanol was used during prehydration. The DPH GCL maintained low hydraulic conductivity ($\approx 10^{-9}$ cm/s) despite permeation with aggressive solutions of strong acid, strong base, and concentrated divalent cations. The improved performance relative to conventional GCLs was attributed mostly to prehydration effects, as well as a smaller contribution from higher bentonite density relative to standard GCLs (6.0 kg/m^2 vs $4\text{-}5 \text{ kg/m}^2$). Intercalation of the Na-CMC was hypothesized to be a significant mechanism, but additional tests with a conventional GCL prehydrated in DI water showed that the intercalation effect could decrease hydraulic conductivity by no more than an order of magnitude (Kolstad et al. 2004b; Tian 2015). Testing was only conducted for less than a year, so the long-term behavior of DPH remains unknown. Other studies have amended bentonite

by hydration in other organic solutions, including propylene carbonate, in order to promote osmotic swelling in highly concentrated solutions (Scalia et al. 2014).

An organic monomer was polymerized in a Na-bentonite slurry by Trauger and Darlington (2000). The material was described as a bentonite-polymer alloy (BPA). The researchers added the slurry to a needle-punched nonwoven geotextile and ran hydraulic conductivity tests with sea water. The resulting hydraulic conductivity was about four magnitudes lower than for a conventional GCL. The polymer was believed to have been bound throughout the montmorillonite interlayer, contributing to the lower hydraulic conductivity. Scalia et al. (2014) followed a similar modification process by using in situ polymerization of acrylic acid to form Na-polyacrylate throughout the interlayer. Polyacrylate had the advantages of being relatively inexpensive, not easily biodegradable, and capable of high swelling and absorption. The resulting material is referred to as bentonite-polymer composite (BPC). The polyacrylate is an anionic polyelectrolyte with a high molecular weight typical of polymers and a strong affinity for water (Schenning 2004). Na-polyacrylate is superabsorbent, capable of absorbing >100 times its mass in water. The behavior and properties of the polymer are related to its structural curling, which is influenced by electrostatic interactions in solution. Complexation, ionic bonding, and coordination to cations at the clay particle surfaces may all contribute to the BPC behavior. Hydraulic conductivity tests were conducted on BPC GCLs to determine their effectiveness as hydraulic barriers in extreme conditions expected from containment systems for mine waste and mineral processing.

Hydraulic conductivity testing by Scalia et al. (2014) showed that BPC GCLs could maintain low hydraulic conductivities with extreme testing conditions for test durations of over two years; however, the mechanism resulting in low hydraulic conductivities was found to be different than for conventional GCLs. The BPC GCLs maintained hydraulic conductivities near 10^{-10} cm/s when permeated with 500 mM CaCl_2 for over two years, whereas conventional GCLs rapidly reached hydraulic conductivities over 10^{-5} cm/s with the same permeant. Solutions of 1 M NaOH

and 1 M HNO₃ yielded similar results, with the BPCs maintaining about 10⁻⁹ cm/s in the long term, as shown in Fig. 2.7.

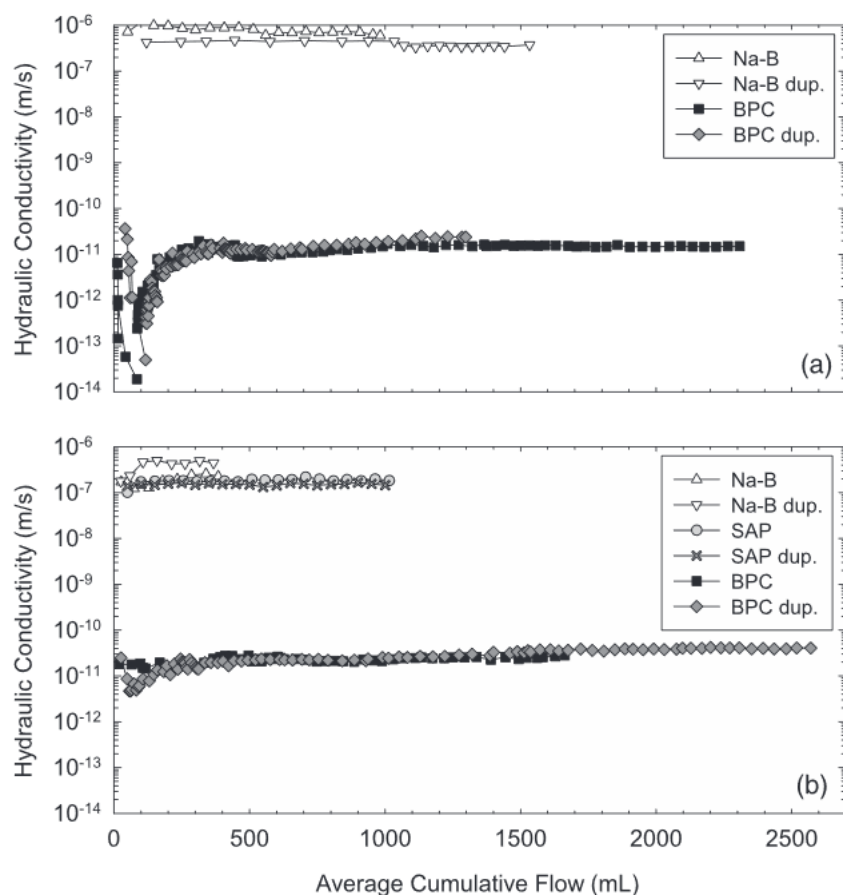


Fig. 2.7. Hydraulic conductivity of BPC GCL relative to conventional GCLs permeated with 1 M NaOH (top) and 1 M HNO₃ (bottom), from Scalia et al. (2014).

Swell index testing of the BPC in the concentrated solutions revealed that the hydraulic conductivity was independent of the swell index. Both BPC and conventional sodium-bentonite experienced very small swell indices in the concentrated solutions, which indicated a lack of osmotic swelling. Therefore, the researchers hypothesized that the mechanism resulting in low hydraulic conductivity for the BPC GCL was different than for conventional Na-bentonite GCL. It was hypothesized that the polyacrylate in the BPC GCL was clogging the pores that would otherwise allow for large hydraulic conductivities. During testing, large amounts of polymer elution

from the BPC GCLs samples was observed. The fraction of polymer eluted from the samples over the entire course of testing was quantified, and it was discovered that polymer elution decreased as the concentration of CaCl_2 in the permeant solution increased (Scalia et al. 2014; Scalia and Benson 2016).

Scalia and Benson (2016) investigated the hydraulic conductivity mechanism of BPC and found evidence of pore clogging by polymer fouling. Polymer elution was again found to decrease with increasing CaCl_2 concentration in the permeant, as shown in Fig. 2.8.

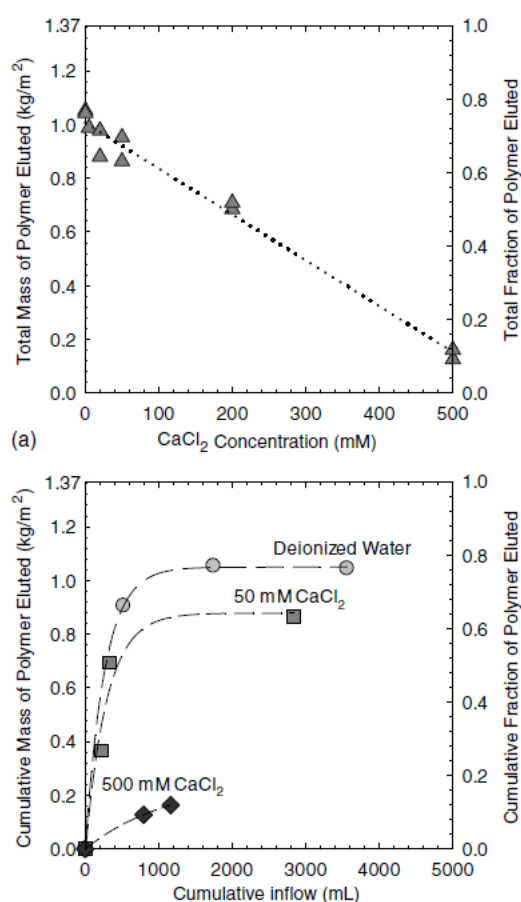


Fig. 2.8. Polymer elution fractions after long term hydraulic conductivity testing with varying CaCl_2 permeant solution strength, from Scalia and Benson (2016).

It was hypothesized that the more concentrated permeants reduced swelling and therefore reduced the size of the pore spaces, increasing the tendency of the polymer to foul pores and

remain within the GCL. Mixtures of sodium bentonite and BPC were found to be effective at reducing the hydraulic conductivity for some types of permeant solutions, and it was noted that permeant specific combinations of the two may be useful in certain applications. Testing with different types of soils showed that the eluted polymer did not reduce the hydraulic conductivity of sand and silt, but clay minerals did experience drops in hydraulic conductivity. Thus, the hydraulic conductivity of clay subgrades below BPC GCLs may be affected by eluted polymer, and more testing will be required to understand the potential effects.

Tian et al. (2017) investigated the effect of varying anion ratio, defined as the ratio of chloride to sulfate by molarity, on the hydraulic conductivity and swell index of a GCL containing a bentonite-polymer mixture. The swell index of the mixture did not vary with anion ratio in a 300 mM Na⁺ solution, but the hydraulic conductivity of the B-P GCL was severely affected. As the anion ratio changed from 0.01 to 100 (chloride: sulfate), the hydraulic conductivity of the B-P GCL increased from approximately 2×10^{-12} m/s to $>10^{-9}$ m/s for a 300 mM Na⁺ permeant solution. Increased polymer elution was observed as the solution became more chloride rich. Solutions with large amounts of chloride are believed to collapse the polymer structure, eliminating its clogging ability and resulting in the opening of preferential flow paths through the pore space. Overall, BPC GCLs are an important research area presenting large possible benefits. Additional research should be focused on studying the useful life expectancy of BPC, the mechanism of pore clogging and its relation to polymer characteristics, and the effect of polymer elution on the subgrade soil.

2.6 Summary of Findings

More investigation is required to fully understand the complex mechanisms of clay-water interaction and the processes of water adsorption and swelling. Still, the results of laboratory testing show that GCLs have good potential to function as effective hydraulic barriers, but the design of the lining system must consider expected field conditions. The lining system should be

designed to avoid the simultaneous occurrence of dehydration and divalent cation exchange within the GCL; the usage of geomembranes and the careful selection of the subgrade soil will aide this objective. In special cases where extreme pH conditions or leachate concentrations are expected, the use of amended bentonites with polymer may be considered. The BPC GCL is particularly promising, but more research is necessary to determine its long-term behavior and the mechanism of its low hydraulic conductivity. Additional research into the field of clay-organic interactions is also required to understand the effects of various types of organic pollutant molecules found in landfills on GCLs. Future GCL alterations may consider methods to reduce the transport of VOCs and other harmful organics.

2.7 References

See end of document.

3 Hydraulic Conductivity of Geosynthetic Clay Liner (GCL) Exhumed from a Composite Liner after 12-yr of Atmospheric Exposure

Abstract: Hydraulic conductivity of a geosynthetic clay liner (GCL) exhumed from a composite liner (geomembrane overlying GCL) in a landfill cell was evaluated after exposure to the atmosphere for 12 yr. The composite liner had been exposed because a leachate collection system had not been placed and the cell was never filled with waste. GCL samples were exhumed from locations along the top, middle, and toe of the east, south, and southeast corner slopes, as well as from the anchor trench. Hydraulic conductivity of the GCL was less than 5.0×10^{-11} m/s or greater than 10^{-7} m/s, depending on sampling location. GCL samples exhumed from the top of slope had low hydraulic conductivities and exhumed water content ($<15\%$) and contained bentonite with relatively high swell index (≥ 20 mL/2 g) and bound cation monovalent mole fraction ($X_M > 0.5$). Samples exhumed from the toe had the high hydraulic conductivities, higher exhumed water contents, low swell index (≤ 11 mL/2 g), low bound cation X_M (≤ 0.12). Hydraulic conductivity of GCLs exhumed from mid-slope and from an anchor trench varied. Five of six GCL samples with low hydraulic conductivity had exhumed gravimetric water contents $< 20\%$, subgrade soil water contents $\leq 5\%$, and a bentonite structure consisting of small granules, suggesting that these GCL samples may have remained relatively dry during the exposure period. The installation of a protective surcharge layer immediately after liner construction is recommended to protect liner material against wet-dry cycling effects.

Key words: Geosynthetic clay liner, hydraulic conductivity, composite liner, bentonite, cation exchange, swell index

3.1 Introduction

Geosynthetic Clay Liners (GCLs) are thin (~10 mm) manufactured hydraulic barriers consisting of bentonite clay and two sheets of geotextile material. The large swelling ability of the bentonite clay in water constricts the pore space available for flow, resulting in low hydraulic conductivity ($\approx 10^{-11}$ m/s) (Shackelford et al. 2000). GCLs are often used in the liner or cover of waste containment systems as part of a composite barrier system. Field investigations into the hydraulic performance of deployed GCLs have found that hydraulic conductivity may increase by several orders of magnitude relative to the installed condition (Benson et al. 2010; Meer and Benson 2007; Scalia and Benson 2010a, 2011). Large increases in field hydraulic conductivity are usually attributed to the rate of polyvalent cation exchange during initial hydration of the GCL and dehydration effects following polyvalent cation exchange.

Cation exchange in a GCL used in a lining system occurs when leachate contacts the bentonite or when cations in the subgrade migrate upward during GCL hydration (Bradshaw et al. 2013, 2015; Bradshaw and Benson 2014). In a composite liner comprised of a geomembrane (GM) over a GCL, the GCL is hydrated primarily by moisture in the underlying subgrade soil. The geochemistry of the subgrade affects the degree of hydration and cation exchange. More concentrated subgrade porewater with a greater proportion of multivalent cations relative to monovalent cations reduces the swelling potential of the bentonite. The chemistry of the permeant solution used during hydraulic conductivity testing influences the swelling potential in the same manner. Thus, the hydration condition and chemistry influence the hydraulic conductivity of GCL (Scalia and Benson 2011).

Hydraulic conductivity of GCLs can also be affected by wet-dry cycling, especially if the GCL undergoes cation exchange and multivalent cations become predominant in the exchange complex of the bentonite. Dehydration of bentonite with a predominantly multivalent exchange complex can permanently remove bound water from the interlayer, resulting in the opening of preferential flow paths during subsequent hydration (Meer and Benson 2007). Several recent

studies have shown that GCLs in composite liners that are left exposed (no leachate collection system or cover soils placed over the liner after construction) are susceptible to wet-dry cycling and subsequent erosion of bentonite within the GCLs (Brachman et al. 2014; Rowe et al. 2016; Take et al. 2015). Sufficient bentonite erosion opened flow channels within the GCLs, undermining their role as hydraulic barriers. In this study, the GCL in a composite liner was exhumed from a landfill cell where the composite liner remained exposed for 12 years because a leachate collection system and waste were not placed. During this exposure period, cation exchange, wet-dry cycling, and erosion of the bentonite in the GCL occurred, affecting the properties of the GCL.

3.2 Background

3.2.1 Relevant Laboratory Testing

Bentonite swelling behavior depends on the hydrating solution characteristics and the bentonite exchange complex (Jo et al. 2001; Kolstad et. al 2004; Meer and Benson 2007; 2009; Scalia and Benson 2010). Jo et al. (2001) showed that Na-bentonite swelling decreased significantly (23-9 mL/2 g) in CaCl_2 solution relative to DI water (35 mL/2 g) as the concentration increased from 10 to 100 mM. Similar decreases were seen for other divalent cation solutions, and the decrease was greatest for a trivalent cation solution (15-8 mL/2 g). Calcium-bentonites, with exchange complexes consisting predominantly of calcium, have less swelling potential in all solutions relative to Na-bentonite, and Ca-bentonite swell in DI water is generally ≤ 10 mL/2 g. Thus, as the proportion of multivalent cations increases in the exchange complex, bentonite swelling potential diminishes. Hydraulic conductivity and swelling share a mechanistic relationship where initial bentonite swelling ability upon permeation is important.

The influence of initial hydration conditions on GCL hydraulic conductivity has been established through laboratory testing (Jo et al. 2004; Petrov and Rowe 1997; Ruhl and Daniel 1997). Direct GCL permeation with moderate concentrations (≈ 50 mM) of polyvalent cations or

large ($\approx >0.5M$) concentrations of monovalent cations usually leads to large hydraulic conductivities relative to DI water near the onset of permeation. Weaker ($<50mM$) multivalent permeant solutions require longer test durations to accurately assess long-term hydraulic conductivity. Jo et al. (2005) showed that permeation with 5 mM $CaCl_2$ increased hydraulic conductivity of GCL by a factor >10 relative to DI water following >100 pore volumes of flow ($\approx 1-2$ yr testing duration). However, initial hydration of the GCL in DW followed by permeation with salt solutions results in lower long-term hydraulic conductivity. It is energetically favorable for the water bound to clay particles during initial osmotic swelling to remain in place despite cation exchange.

Na-bentonite undergoing cation exchange with multivalent cations in solution is susceptible to repeated cycles of wetting and drying. Drying of the bentonite removes previously bound water, and adequate swelling is required upon rehydration to avoid potentially large increases in hydraulic conductivity. Azad et al. (2011) showed that GCL wet-dry cycling in deionized water did not significantly affect the hydraulic conductivity, but Lin and Benson (2000) established that wet-dry cycling of GCL with a dilute calcium solution (12.5 mM $CaCl_2$) could raise the hydraulic conductivity of GCL by over three orders of magnitude within five wet-dry cycles. The cycling accelerated polyvalent cation exchange, eventually reducing the swelling potential of the bentonite enough to preclude the healing of desiccation cracks. Benson and Meer (2009) noted that the relative abundance of monovalent and divalent cations (RMD) in hydrating solutions influenced the effect of wet-dry cycling; solutions with greater abundance of divalent cations experienced more rapid and severe decreases in swelling potential.

3.2.2 Previous Exhumed GCL Studies

James et al. (1997) exhumed GCL used in a sealing application with an overlying gravel layer (150 mm) and cover soil (300 mm). Fine cracking of the GCL was observed, and GCL testing showed high moisture contents and significant exchange of sodium for calcium in the bentonite exchange complex. The calcium source was attributed to calcite in the GCL bentonite and

overlying soil. An experiment was designed to estimate the rate of new GCL cation exchange under field conditions. Water was flowed horizontally through a gravel layer overlying new GCL and collected at an outlet. A small vertical flow through the GCL was observed at the start of testing but stopped after 3 hours despite a hydraulic gradient of 150 imposed on the GCL. The GCL permeability was concluded to have not changed after a 16 hr test duration, and subsequent testing of the bentonite exchange complex showed that Na exchange by Ca was minor. The permeability of the exhumed GCL was not tested. Wagner and Schnatmeyer (2002) conducted inclined (5%) field tests of different sealing systems with an overlying covering layer (750 mm). Covered GCL maintained $k < 5 \times 10^{-9}$ m/s, meeting regulatory requirements, whereas an uncovered clay liner failed due to desiccation. The GCL was noted to be subject to deterioration from aging, and the hydraulic conductivity increased during the 2-yr observation period. Cation exchange was believed to be in progress, and a final evaluation of the long-term GCL hydraulic conductivity could not be made.

Meer and Benson (2007) studied exhumed GCL from varying landfill final covers, including composite and non-composite barriers, at multiple sites. Soil cover at each site varied between 750-900 mm. The exhumed water contents of GCL with no overlying GM varied between 31-59% for the driest site and 166-204% for the wettest site (site D). Exhumed water content with overlying GM varied between 58-61% (site S). Extensive exchange of sodium for magnesium and calcium was recorded for all exhumed GCL ($X_{Na} < 0.29$) regardless of GM presence. Swell indices for select GCL from each site varied between 8-11 mL/2 g. Hydraulic conductivity testing was conducted with 10 mL $CaCl_2$, and the median hydraulic conductivity was $< 10^{-5}$ cm/s for only the wettest site (site D, median $K = 5.5 \times 10^{-8}$ cm/s). Site D maintained relatively low hydraulic conductivity despite extensive multivalent cation exchange. The overlying GM did not protect site S from multivalent cation exchange nor increased hydraulic conductivity ($> 10^{-5}$ cm/s). Controlled desiccation of the wet GCL specimens from site D found that drying to water contents $< 100\%$

resulted in 3-4 order of magnitude increases in hydraulic conductivity, demonstrating the adverse effects of wet-dry cycling on exchanged bentonite.

Scalia and Benson (2010) showed that the choice of permeant water used during hydraulic conductivity testing greatly influenced the permeability of exhumed GCL, even if the solutions were dilute ($\leq 10\text{mM}$). Deionized water (DI), 0.01M CaCl_2 (SW), and “average water” (AW) with 0.3mM NaCl and 1.9mM CaCl_2 were used. Exhumed GCL with water content $>53\%$ maintained $k < 5 \times 10^{-11} \text{ m/s}$ for all solutions, and GCL with lower water contents showed higher hydraulic conductivities (2-4 orders of magnitude) to SW relative to AW or DW. However, the presence of macroscopic features in the exhumed GCL affected this trend. Macroscopic features, such as preferential flow paths along fibers, resulted in similar hydraulic conductivities to SW and AW but decreased permeability with DI. Scalia and Benson (2011) showed that porewater chemistry and water content of the subgrade soil influenced the hydraulic properties of exhumed GCL. Subgrade soils with water contents in excess of optimum corresponded to GCLs with larger exhumed water contents and lower hydraulic conductivities. Exhumed GCLs which lacked preferential flow paths and had low hydraulic conductivities were associated with subgrades having low concentrations of soluble cations.

3.3 Exhumation and Test Methods

3.3.1 Exhumation of GCL

GCL samples were obtained from a composite liner along the side slopes (2:1 slope, 26.6°) in an unused cell at a municipal solid waste landfill located in a temperate climate zone (Csb - temperate, dry summer, warm summer, Peel et al. (2007)) in California. Samples were exhumed from southern and eastern slopes near top of slope, mid-slope, and toe (bottom) of slope. Samples were also exhumed from the anchor trench (A1 and A2). A plan view of relative GCL exhumation locations is shown in Fig. 3.1, and GCL sample designations are shown in Table

3.1. The GCL was needle punched with nonwoven cover and carrier geotextiles and originally contained granular Na-bentonite.

3.3.2 Hydraulic Conductivity

Hydraulic conductivity testing of the exhumed GCL was completed in flexible wall permeameter cells in accordance with ASTM 5084-16a Method B. No backpressure was applied to simulate the field condition as in previous exhumed GCL studies (Meer and Benson 2007; Scalia and Benson 2011). A hydraulic gradient between 100-320 and average effective stress of 21 kPa was applied. The hydraulic gradient used is greater than that experienced in the field, but previous laboratory testing shows that varying hydraulic gradient has a modest effect on GCL hydraulic conductivity relative to the effective stress (Petrov et al. 1997a; b). The seepage induced consolidation introduced by varying hydraulic gradient over the short length of the GCL is small, and the use of large hydraulic gradients allowed testing to be conducted over a suitable time period.

Scalia and Benson (2010) showed that permeant water chemistry can affect the hydraulic conductivity of exhumed GCL by multiple orders of magnitude relative to DW even if the solution is dilute (≤ 10 mM CaCl_2). The selection of a permeant water resembling the typical field conditions was recommended to assess hydraulic conductivity. Herein, the subgrade soil porewater chemistry was unknown at the onset of hydraulic conductivity testing, so a solution of 1.3 mM NaCl and 0.8 mM CaCl_2 , named Average Water (AW), was used. The AW solution (73.8 mg NaCl and 87.0 mg CaCl_2) was designed to simulate typical porewater chemistry in cover soils placed adjacent to GCLs.

GCL specimens for hydraulic conductivity testing were extracted from the GCL sample using a razor knife. The perimeter of the specimen was wetted with a small volume of permeant liquid during the extraction to reduce the loss of bentonite. Frayed geotextile fibers were cut away with scissors. To discourage sidewall leakage, bentonite paste was applied around the edge of

the specimen. Calipers were used to estimate the thickness of the specimen before and after testing. Permeation of the specimens was continued until at least four steady values of hydraulic conductivity ($\pm 25\%$ of the mean) were obtained over a time duration where the ratio of outflow to inflow was between 0.75 and 1.25.

Hydraulic conductivities are listed in Table 3.1. Time-varying behavior was noted during testing, and general trends are shown in Fig. 3.2. The majority of GCL specimens maintained a steady hydraulic conductivity throughout testing. Decreasing hydraulic conductivity was observed in two specimens, but no increasing trends. All specimens with final hydraulic conductivity $\geq 10^{-7}$ m/s were tested for sidewall leakage by adding rhodamine WT dye to the permeant liquid. After termination, the GCL specimens were examined to determine the flow path and ensure that sidewall leakage did not occur.

3.3.3 Swell Index

The swell index of the exhumed GCL contents was measured following ASTM 5890-11, using 2.0 g of oven dried and finely ground (passing #200 sieve) material. Deionized water was used as the testing reagent. SI are listed in Table 3.1.

3.3.4 Mass per Area

Mass per area measurements were conducted in accordance with ASTM D5993-14. Square specimens with 100 mm side length were cut from the exhumed GCL using a razor. The specimen perimeter was wetted to limit clay granule loss during cutting. One specimen was cut per GCL sample, and the resulting measurements of the whole GCL mass per unit area are listed in Table 3.1.

3.3.5 XRD

X-ray diffraction was conducted by Mineralogy, Inc. (Tulsa, Oklahoma) using a method modified from Moore and Reynolds (1989) to determine the mineralogy of selected exhumed GCL

and subgrade soil samples. Table 3.1 lists the montmorillonite fraction of select GCL samples and Table 3.2 details the subgrade soil. The preparation of XRD samples included grinding with a mortar and pestle, dispersion in dilute sodium phosphate solution using a sonic probe, vacuum-depositing on nylon membrane filters, attachment to glass slides, and exposure to ethylene glycol vapor for 24 h. A Rigaku Ultima IV XRD system was used, and quantitative analysis employed the Rietveld method.

3.3.6 Bentonite Exchange Complex

Measurements of soluble cations, bound cations, and cation exchange capacities (CEC) were completed in accordance with ASTM D7503-10. Contents of the exhumed GCL samples were extracted from an area near the hydraulic conductivity specimen, oven dried at 110°C, and ground to pass a #10 sieve. Type II DI water, 1.0 M NH₄OAc, and 1.0 M KCl solutions were used respectively for soluble cations, bound cations, and CEC. Inductively coupled plasma mass spectrometry (ICP-MS) was completed using an Agilent 7900 Quadrupole ICP-MS to measure the major cation concentrations (Na, K, Ca, Mg) in vacuum filtered extracts. The extracts were prepared for ICP-MS analysis by filtering at 0.45 µm and acidifying with trace metal grade nitric acid to pH = 2. The total soluble cation charge per mass (Table 3.3) was calculated by summing the major cation concentrations. CEC was measured by determining the concentration of ammonium extracted from the specimen exchange complex with 1.0 M KCl. NH₃-N concentrations were measured with a Hach DR6000 spectrophotometer using the salicylate method. A 100 mg/L ammonia standard solution was used to ensure the spectrophotometer calibration. Table 3.1 shows the monovalent mole fraction (X_M) of the major bound cations on the exhumed GCL contents (calculated as the sodium and potassium charge per mass relative to the total CEC charge per mass).

3.4 Results and Discussion

3.4.1 Exhumed Condition of GCL

Visual inspection showed varying states of hydration of the exhumed GCL as shown in Fig. 3.3. GCL exhumed from slope top and mid-slope positions contained small granules as in Fig. 3.3 (b) while samples from slope toe positions showed either a gel-like structure Fig. 3.3 (d) or apparent desiccation cracking Fig. 3.3(c). GCL exhumed from the anchor trench sample contained larger granules (Fig. 3.3a) relative to the top slope and mid-slope samples, and water content testing showed the anchor trench was wetter (34%, Fig. 3.4) than the mean of the top slope and mid slope exhumed GCL (13%) but dryer than the mean of the slope toe (50%). The mid-slope and top-slope GCL and subgrade soil water contents (average = 1.9%) are low relative to previous studies. Yet, the range of exhumed GCL water contents reported within (2-86%) exceeds that reported in Meer and Benson (2007), Scalia and Benson (2011), and Benson, Kucukkirca, and Scalia (2010) for final cover exhumed GCL with overlying GM and cover soil (57.9-60.8%, 17-70%, and 56-70% respectively). Meer and Benson (2007) recorded a larger range (31-204%) and average of exhumed water contents in the case of GCL with cover soil and no GM.

The swell index of the exhumed GCL and the monovalent mole fraction (X_M) of the major bound cations shared a decreasing trend down the slope length (Fig. 3.4). The slope-top GCLs had significantly larger swell indices and bound cation X_M than the slope-toe samples which corresponded to calcium bentonite (22 vs. 9 mL/2 g, 0.63 vs. 0.06). Variance was greatest at mid-slope (10-20 mL/2 g, 0.15-0.61). The anchor trench values were intermediate (average 13 mL/2g and 0.3) despite the protective presence of cover soil. SI and bound cation X_M from anchor trench specimens separated by approximately 300 mm showed significant variance (11-16 mL/2 g and 0.22-0.38), indicating that localized effects are important. The swelling potential of all exhumed GCL diminished relative to the manufacturer's reported 24 mL/2g excepting PS-T which had the lowest exhumed water content after the severely eroded SS-B sample. The observed replacement of sodium with polyvalent cations in the exhumed GCL exchange complex confirms

previous field studies showing that hydration by soil porewater leads to long-term multivalent cation exchange (Meer and Benson 2007; Scalia et al. 2017; Scalia and Benson 2011).

The exhumed GCL water content exhibited a proportional relationship with the subgrade soil water content in all cases except for the severely eroded SS-B GCL (Fig. 3.5a). The presence of the overlying GM limits the moisture source of the GCL to the subgrade soil, but the lack of protective cover over the GM may inhibit sustained hydration through severe temperature cycling, as observed in the QUELTS I and II field tests (Brachman et al. 2014; Rowe et al. 2014, 2016). A cluster of exhumed GCL with subgrade soil and exhumed GCL water contents less than 2% and 16%, respectively, is noted in Fig. 3.5a. The cluster retained bound $X_M > 0.5$ and $SI > 18$ mL/2g, and visual inspection of the cluster showed granular bentonite Fig. 3.3b. The exhumed water content, exchange complex composition, and visual condition of the exhumed GCL cluster suggest that GCL hydration was sufficiently limited to preclude osmotic swelling and reduce the rate of multivalent cation exchange during the exposure period. Decreased montmorillonite content of the exhumed GCL due to erosion was also considered as a cause of varying SI and bound cation X_M , but XRD testing of 7 specimens from varying locations showed a narrow range of MMT contents (73-82%) that did not correlate with SI , excluding the severely eroded SS-B GCL (Fig. 3.5b).

3.4.2 Hydraulic Conductivity of Exhumed GCL

Hydraulic conductivity to average water of the exhumed GCL relative to slope position is shown in Fig. 3.6. Exhumed GCL from slope-top positions maintained low hydraulic conductivities ($< 5 \times 10^{-11}$ m/s), and all slope-toe samples exceeded 10^{-7} m/s. Mid-slope samples and the adjacent anchor trench specimens varied in hydraulic conductivity by up to five orders of magnitude (10^{-6} m/s vs. 10^{-11} m/s). Comparison of GCL mass per area and hydraulic conductivity shows no apparent trend (Table 3.1) except for SS-B which eroded sufficiently to ruin the GCL integrity. Swell indices of the exhumed bentonite appear indicative of the hydraulic conductivity

(Fig. 3.7a), which contrasts with the ranges of hydraulic conductivities (varying by up to four orders of magnitude) recorded at given swell values in Meer and Benson (2007) and Scalia and Benson (2011) for DW and SW permeant solutions. The use of SW (10mM CaCl_2) for hydraulic conductivity testing in these studies restricted the swelling ability of the exhumed GCL to a greater degree than the AW solution herein, as shown by Scalia IV and Benson (2010) for a range of exhumed GCL with intermediate SI (10-20 mL/2 g). Reflecting previous studies, the bound cation X_M determined the SI in DW (Fig. 3.7b). All exhumed GCL with bound cation $X_M \geq 0.38$ swelled adequately in AW to achieve low hydraulic conductivity. The water content of the exhumed GCL following hydraulic conductivity testing is determined by the swelling ability of the bentonite in AW. Large post testing water contents (>120%) are associated with larger bound cation X_M and osmotic swelling of the bentonite. Insufficient swelling leads to lower post-testing water contents (<100%) and failure to block pores which control hydraulic conductivity. Preferential flow channels enabled large increases in hydraulic conductivity when swelling was inadequate.

Field studies of exhumed GCL suggest that polyvalent cation exchange is inevitable in the long term. However, low hydraulic conductivity of GCL may be achieved if sufficient hydration occurs initially and is continuously maintained during polyvalent cation exchange (Jo et al. 2004). A comparison of the exhumed GCL bound cation X_M with the exhumed water content (Fig. 3.9a) shows that moisture availability results in the bentonite undergoing multivalent cation exchange with soil porewater. The cluster of samples with low exhumed water content (<16%) and high bound cation X_M (>0.5) suggests that the GCL remained dry enough to diminish the effect of cation exchange, but a low exhumed water content does not guarantee avoidance of polyvalent exchange. The relationship between hydraulic conductivity and exhumed water content shown in Fig. 3.9b also suggests that some GCLs maintained sufficiently dry conditions to avoid cation exchange and maintain low hydraulic conductivity. Contrary to the typical case for landfill final covers, most of the exhumed GCL with larger water contents (>16%) had higher hydraulic conductivities (> 10^{-7} m/s). All exhumed GCL specimens with apparent visual evidence of

desiccation cracking belonged to the high hydraulic conductivity, suggesting that susceptibility to wet-dry cycling affected the exhumed GCL condition.

3.4.3 Influence of Subgrade Porewater Chemistry

Subgrade soils with low total soluble cation charge per mass (TCM) and adequate moisture availability were shown to promote low hydraulic conductivity of exhumed GCL from a landfill cover to DW and 10mM CaCl₂ by Scalia and Benson (2011). Varying subgrade soil porewater chemistry may influence the extent and rate of polyvalent cation exchange, which can affect the hydraulic conductivity of exhumed GCL. Table 3.3 details the average subgrade TCM, monovalent mole fraction (X_M) of soluble cations, GCL TCM, and GCL soluble cations X_M by slope position. The average subgrade soil TCM and GCL TCM are significantly lower for the slope-toe samples (1.3 cmol⁺/kg and 3.0 cmol⁺/kg) relative to the other positions, but the soluble cations X_M does not have a positional trend. The lack of a clear relationship between GCL bound cations X_M and subgrade TCM is shown in Fig. 3.10a. The samples with $X_M > 0.5$ had low hydraulic conductivities but varied widely (1-7 cmol⁺/kg) in subgrade soil TCM.

Comparing the GCL TCM with the subgrade TCM showed no direct relationship between the two (Fig. 3.10b) in contrast to the findings of Scalia and Benson (2011). There is a relationship between GCL TCM and hydraulic conductivity. Hydraulic conductivities were consistently low for GCL TCM > 15 cmol⁺/kg and consistently high for GCL TCM < 5 cmol⁺/kg, whereas Scalia and Benson (2011) found low hydraulic conductivity to be obtained for GCL TCM ≤ 7 cmol⁺/kg. The lack of a clear relationship between GCL TCM and subgrade TCM may relate to the varying extents of hydration of the GCL. The cluster of slope-toe samples with low subgrade TCM and low GCL TCM had the greatest exhumed water contents (average = 50%), indicating sufficient moisture availability for exchange between the subgrade and GCL porewater. The exhumed water content was < 15% for all GCLs with TCM > 20.0 cmol⁺/kg. Considering the granular structure of the bentonite from the GCL with TCM > 20.0 cmol⁺/kg, moisture availability may have limited

exchange between the subgrade and GCL porewater. Exchange complex testing of new GCL product comparable to the exhumed GCL gave $TCM = 32.0 \text{ cmol}^+/\text{kg}$ with $X_M = 0.97$, indicating that exhumed GCL with $TCM > 20.0 \text{ cmol}^+/\text{kg}$ is most similar to the new GCL condition.

The exhumed GCL TCM and subgrade soil water content appear to have an inversely proportional relationship (Fig. 3.11a) which reflects observations from Scalia and Benson (2011). GCL TCM was $> 20.0 \text{ cmol}^+/\text{kg}$ for subgrade water content $< 2\%$, and the GCL TCM varied between 2.4-14 cmol^+/kg for subgrade water contents between 2-10%. The cluster of exhumed GCL with $TCM > 20.0 \text{ cmol}^+/\text{kg}$ shows that low moisture availability enabled bound cation $X_M > 0.5$ and $K < 4.0 \times 10^{-11} \text{ m/s}$. The inversely proportional relationship between GCL bound cation X_M and the subgrade soil water content is shown in Fig. 3.11b.

3.4.4 Desiccation Effects and Preferential Flow

Rowe et al. (2016) established through a field experiment that an exposed black geomembrane (GM) reaches temperatures up to 60-70 °C on sunny days. The temperature cycling of the overlying black GM likely affected the GCL ability to sustain hydration and promoted wet-dry cycling of the GCL (Azad et al. 2011). Excluding the covered anchor trench samples, the average subgrade water content was 7.6% for hydraulic conductivity $> 10^{-7} \text{ m/s}$ and 1.8% for $< 5 \times 10^{-11} \text{ m/s}$, indicating that subgrade moisture availability did not promote low hydraulic conductivity. Rather, moisture availability may have promoted wet-dry cycling, and two of the three slope samples with the largest subgrade water contents visually showed desiccation cracking (SS-B Seam and ES-B Fig. 3.12 (a) and (b)). Previous exhumed GCL studies show that GCL specimens which underwent and maintained significant hydration may maintain low hydraulic conductivity despite extensive polyvalent cation exchange (Meer and Benson 2007; Scalia and Benson 2010a). One exhumed GCL sample herein visually showed a gel-like structure suggestive of sustained osmotic swelling (SE-B, $w = 86\%$). Permeation of SE-B yielded hydraulic conductivity $> 10^{-7} \text{ m/s}$, and dye testing revealed preferential flow along a bundle of needle-

punched fibers (Fig. 3.12d), indicating that bentonite swelling was insufficient near the fibers to close the flow channel.

3.5 Summary and Conclusions

The effects of a 12-yr atmospheric exposure on GCL in an uncovered composite landfill liner (GM over GCL) were examined. GCL was exhumed from the east, southeast, and south slope of the landfill, and from varying locations along the slope length (anchor, top, mid-slope, toe/bottom). The exhumed GCL condition was assessed by measuring water content, swell index, mass per area, exchange complex composition, and hydraulic conductivity. Testing of exhumed GCL showed spatial trends with location along the slope length, and hydraulic conductivity testing showed two distinct behaviors ($k > 10^{-7}$ m/s or $k < 5 \times 10^{-11}$ m/s). Key findings and recommendations are presented.

1. The properties and appearance of top and mid-slope samples most closely resembled new GCL. Excepting sample ES-M, GCL from these slope locations consistently had low exhumed water contents ($\leq 15\%$), predominantly monovalent exchange complexes ($X_M > 0.5$), larger TCM (> 14 cmol+/kg), and low hydraulic conductivities ($< 5 \times 10^{-11}$ m/s). Evidence suggested that top slope GCL samples did not hydrate significantly during the exposure period and avoided severe wet-dry cycling effects.
2. Slope bottom/toe samples showed the most severe degradation. Exhumed GCL properties least resembled new GCL, having swell indices < 11 mL/2 g, bound cation $X_M < 0.2$, and hydraulic conductivities $> 10^{-7}$ m/s. Desiccation cracking was visually apparent upon exhumation at two locations, and severe erosion was noted at a third. Only one exhumed GCL showed a gel-like structure, but it had a preferential flow channel.
3. For typical conditions, a GCL would ideally be installed on a subgrade soil wet of optimum to promote and sustain adequate hydration. However, a moist subgrade soil may become problematic for an uncovered composite liner (GM over GCL). Wet-dry cycling induced by

varying GM temperatures may accelerate degradation for GCL with moisture availability. Therefore, quickly installing protective cover over composite barriers with moist subgrades should be prioritized.

4. Subgrade soil porewater chemistry did not directly correlate with the composition of the bentonite exchange complex for the exhumed GCL. The lack of significant hydration appears to have reduced exchange with subgrade porewater for top and mid slope samples. Exhumed GCL and subgrade soils from the slope bottom had low TCM and the least variance, suggesting greater exchange with the subgrade porewater.
5. The timely installation of a protective ballast layer is necessary to protect the longevity of composite liner systems.

3.6 Acknowledgement

Financial support for this study was provided by the US Department of Energy (DOE) under cooperative agreement DE-FC01-06EW07053 entitled the Consortium for Risk Evaluation with Stakeholder Participation III and the Global Waste Research Institute at California Polytechnic State University. Collaboration of Waste Connections, Inc. and cooperation of the partner landfill is appreciated.

3.7 References

See end of document.

3.8 Tables and Figures

Table 3.1. Characteristics of exhumed GCL samples.

GCL Sample ID ^a	GCL Water Content (%)	Subgrade Water Content (%)	GCL Mass Per Area (kg/m ²) ^b	MMT ^c Content (%)	Swell Index (mL/2 g)	Hydraulic Conductivity (m/s)	Post-Permeation Water Content (%)	Monovalent Mole Fraction of Bound Cations on Bentonite (X_M)
New GCL			4.4 ^d		24 ^d	5.0×10^{-11} ^d		
ES-T	14	5.0	4.5	78	20	3.9×10^{-11}	148	0.56
ES-M	14	2.4	6.2	75	10.0	2.6×10^{-6}	77	0.15
ES-B	39	8.5	4.9	79	10.0	1.3×10^{-6}	98	0.03
SS-T	13	1.1	4.4	NM	22.0	2.5×10^{-11}	184	0.64
SS-M	11	1.1	6.1	NM	20.0	3.1×10^{-11}	151	0.61
SS-B	2	4.4	1.6	57	3.0	2.6×10^{-6}	NM	NM
SE-T	15	0.8	4.5	81	23.0	2.9×10^{-11}	163	0.65
SE-M	14	1.3	4.8	73	18.5	2.4×10^{-11}	124	0.56
SE-B	86	16	5.8	82	8.0	3.1×10^{-7}	99.5	0.02
A1	32	8.1	5.4	78	11.0	1.2×10^{-6}	91	0.22
A2	37	8.1	5.2	NM	16.0	3.9×10^{-11}	133	0.38
PS-T	10	1.4		NM	24.0	9.7×10^{-12}	133	0.66
SS-B, Seam Overlap	25	6.5	NM	NM	10.5	2.1×10^{-7}	81	0.12

^aES = east slope, SS = south slope, A = anchor trench, SE = southeast corner slope, T = top, M = middle, B = bottom, PS = panel separation; ^bincludes geotextiles and bentonite, initial mass per unit area of installed GCL ~ 5 kg/m²; ^cMMT = Montmorillonite. NM indicates not measured; ^dReported by manufacturer.

Table 3.2. Major mineral constituents of subgrade soil samples determined from X-Ray diffraction (n=14). X-Ray diffraction testing was performed by Mineralogy-Inc.

Slope ID	Location along slope length	Major Mineral Constituents (%)				
		Quartz	Plagioclase Feldspar	Microcline	Montmorillonite	Other
East	Top	40	38	12	8	2
East	Middle	36	38	12	10	4
East	Bottom	35	37	13	10	5
Southeast	Middle	34	38	13	14	1
South	Bottom	36	34	15	10	5

Table 3.3. Average subgrade water content and soluble cation properties relative to location along slope

Location	Subgrade Water Content (%)		Subgrade TCM ^a (cmol ⁺ /kg)		Subgrade Soluble Cations, X _M ^b		GCL TCM (cmol ⁺ /kg)		GCL Soluble Cations, X _M	
	Mean	Std. dev.	Mean	Std. dev.	Mean	Std. dev.	Mean	Std. dev.	Mean	Std. dev.
Anchor	8.1		3.7		0.6		12.6	1.1	0.7	0.1
Top	2.1	1.7	3.4	2.5	0.8	0.1	20.5	3.5	0.9	0.1
Middle	1.6	0.6	3.9	2.1	0.7	0.1	21.9	7.1	0.9	0.0
Bottom	9.0	4.6	1.3	0.4	0.7	0.2	3.0	0.9	0.7	0.2

^aTCM = total charge of major soluble cations per mass of soil solids

^bX_M = Monovalent mole fraction of major cations

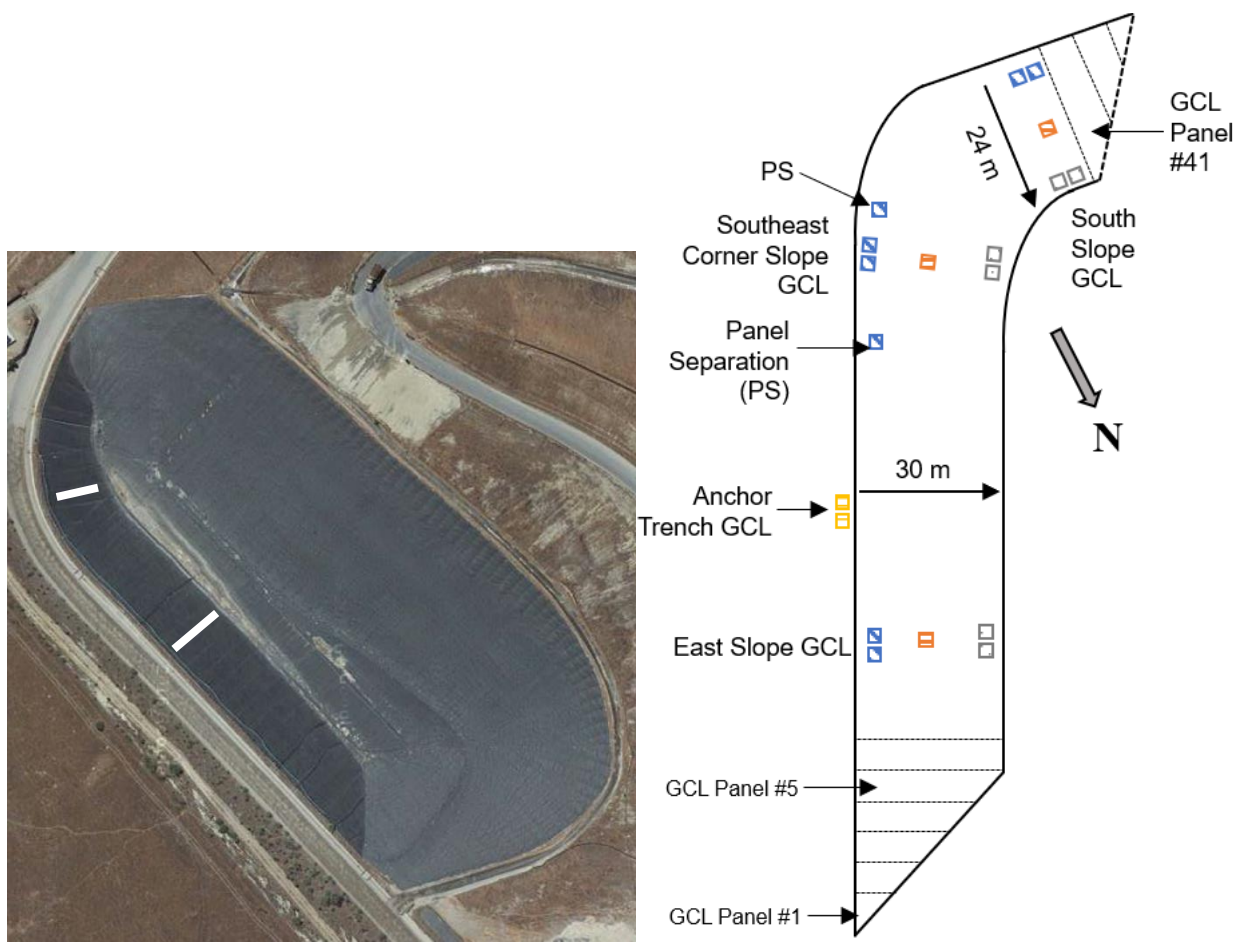


Fig. 3.1. Overhead aerial image of landfill site (left), courtesy of Professor Jim Hanson at Cal Poly San Luis Obispo. White lines indicate approximate exhumation locations of the east and southeast corner slopes. Plan view of landfill slope and locations of GCL sample exhumation (right). Drawing is not to scale. Colored squares indicate GCL exhumation positions. Color corresponds to location along slope (top=blue, middle=orange, bottom/toe=gray, anchor=yellow).

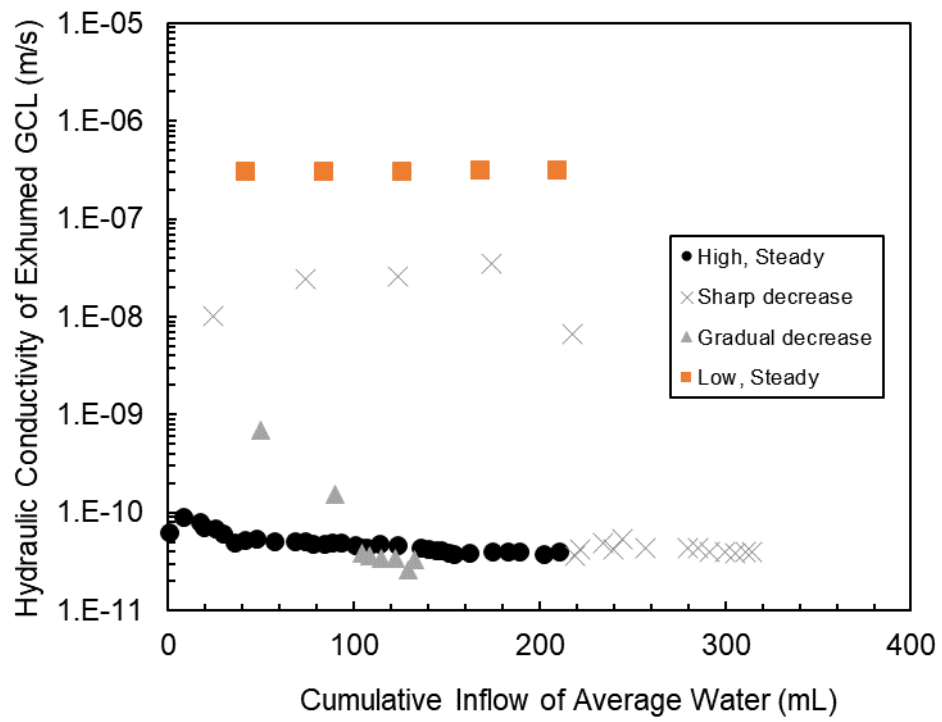


Fig. 3.2. Overview of hydraulic conductivity behavior during testing of the exhumed GCL.

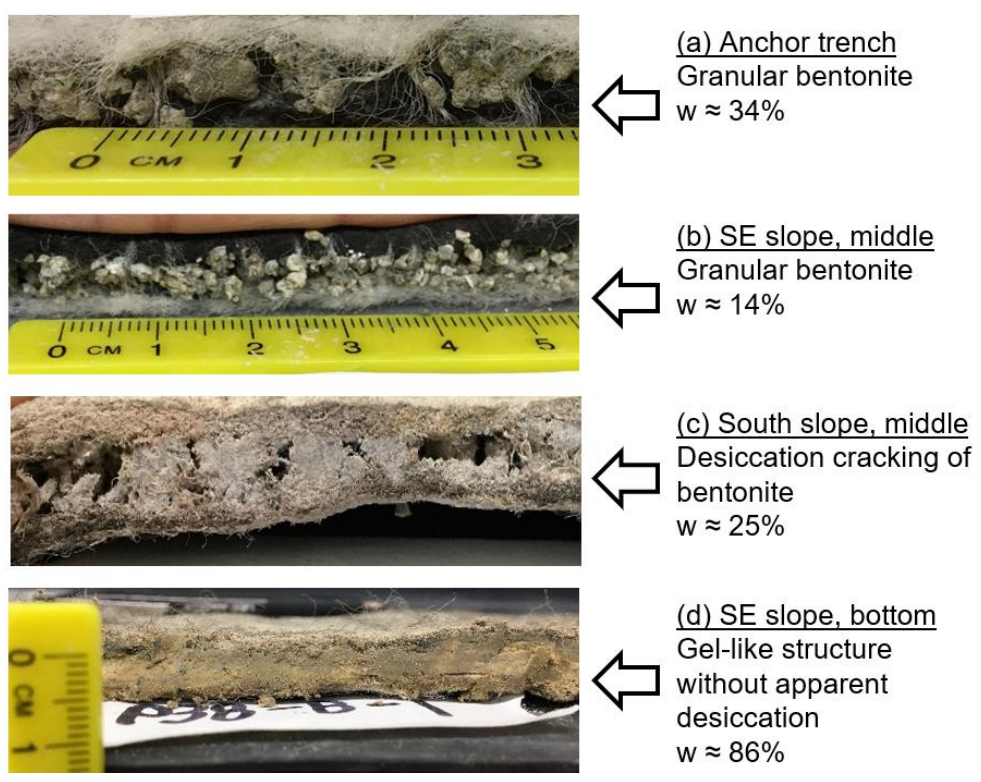


Fig. 3.3. Exhumed GCL with varying gravimetric water content. The initial condition of the exhumed bentonite varies between gel-like, desiccated, and granular.

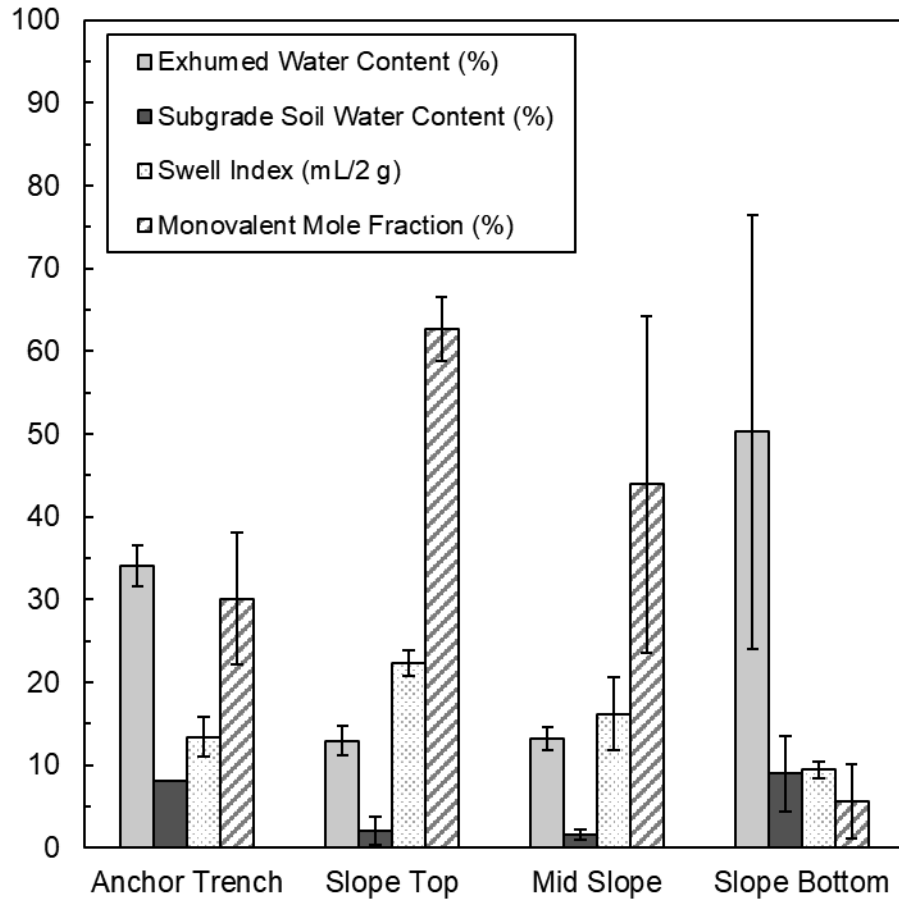


Fig. 3.4. Average properties of exhumed GCL from varying slope positions. The gravimetric water content was measured using the internal contents of the GCL. The monovalent mole fraction refers to the major bound cation composition of the exhumed bentonite.

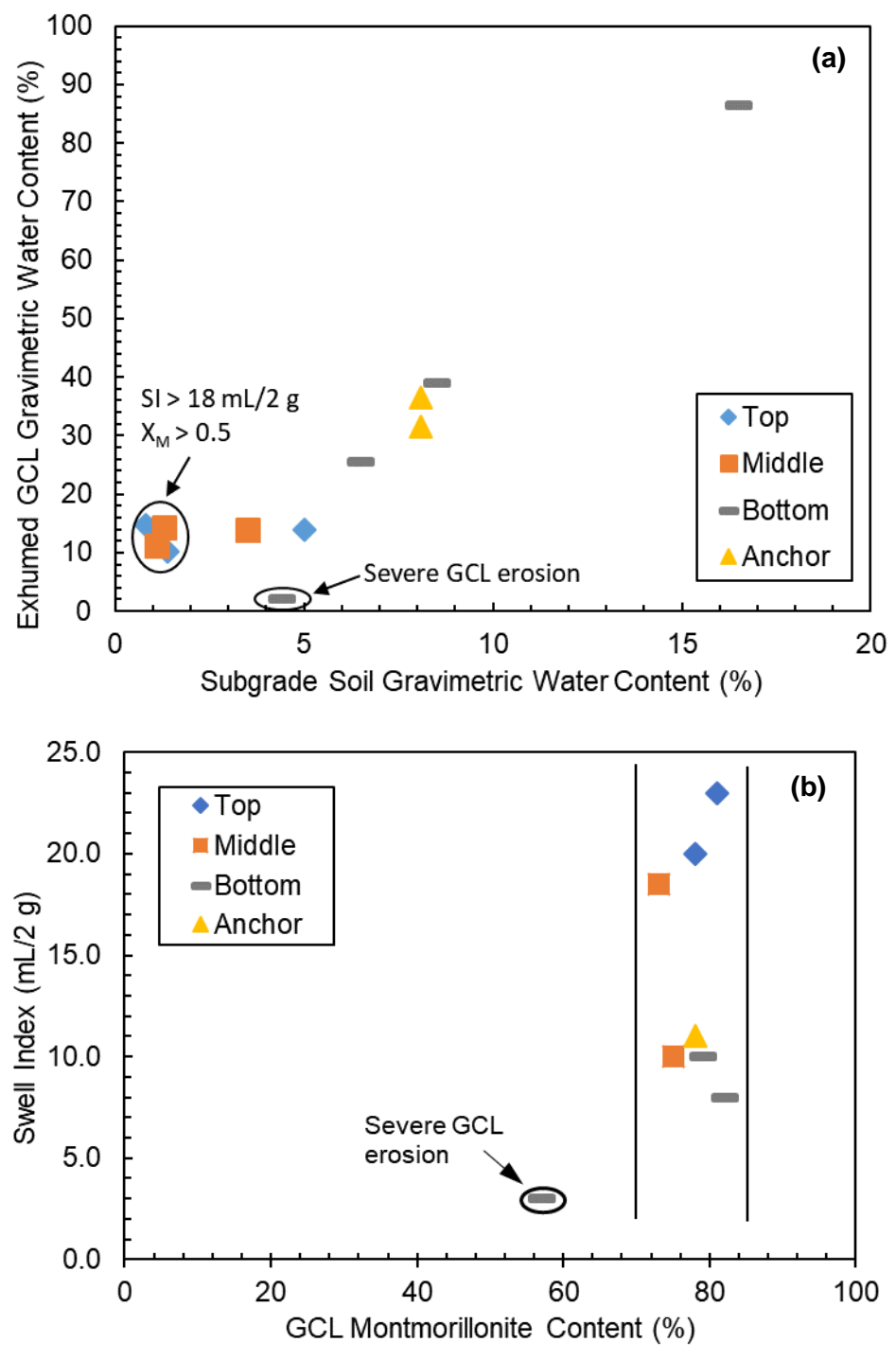


Fig. 3.5. Exhumed GCL gravimetric water content vs. subgrade soil gravimetric water content (a) and the swell index of the exhumed GCL versus the montmorillonite content. ES = east slope.

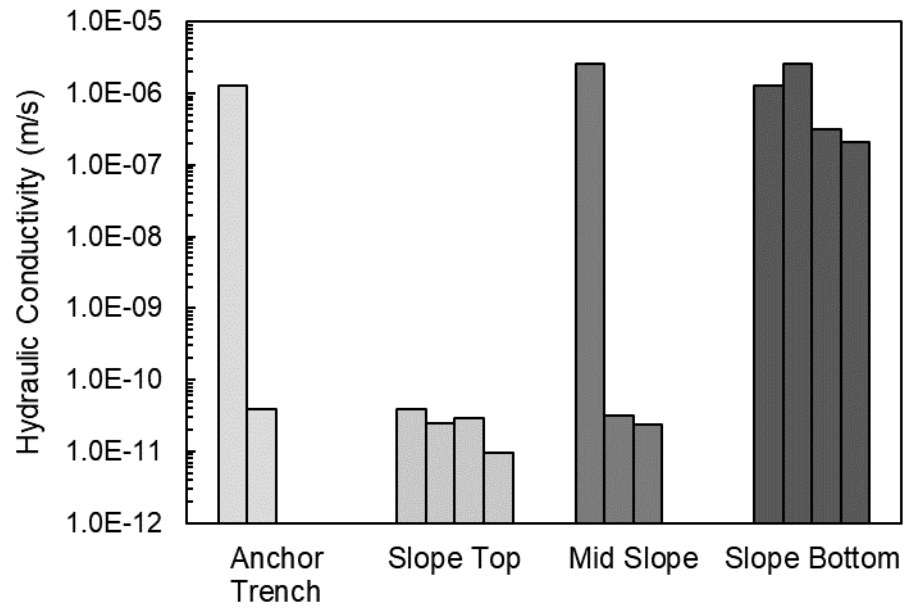


Fig. 3.6. Hydraulic conductivity with average water versus slope location.

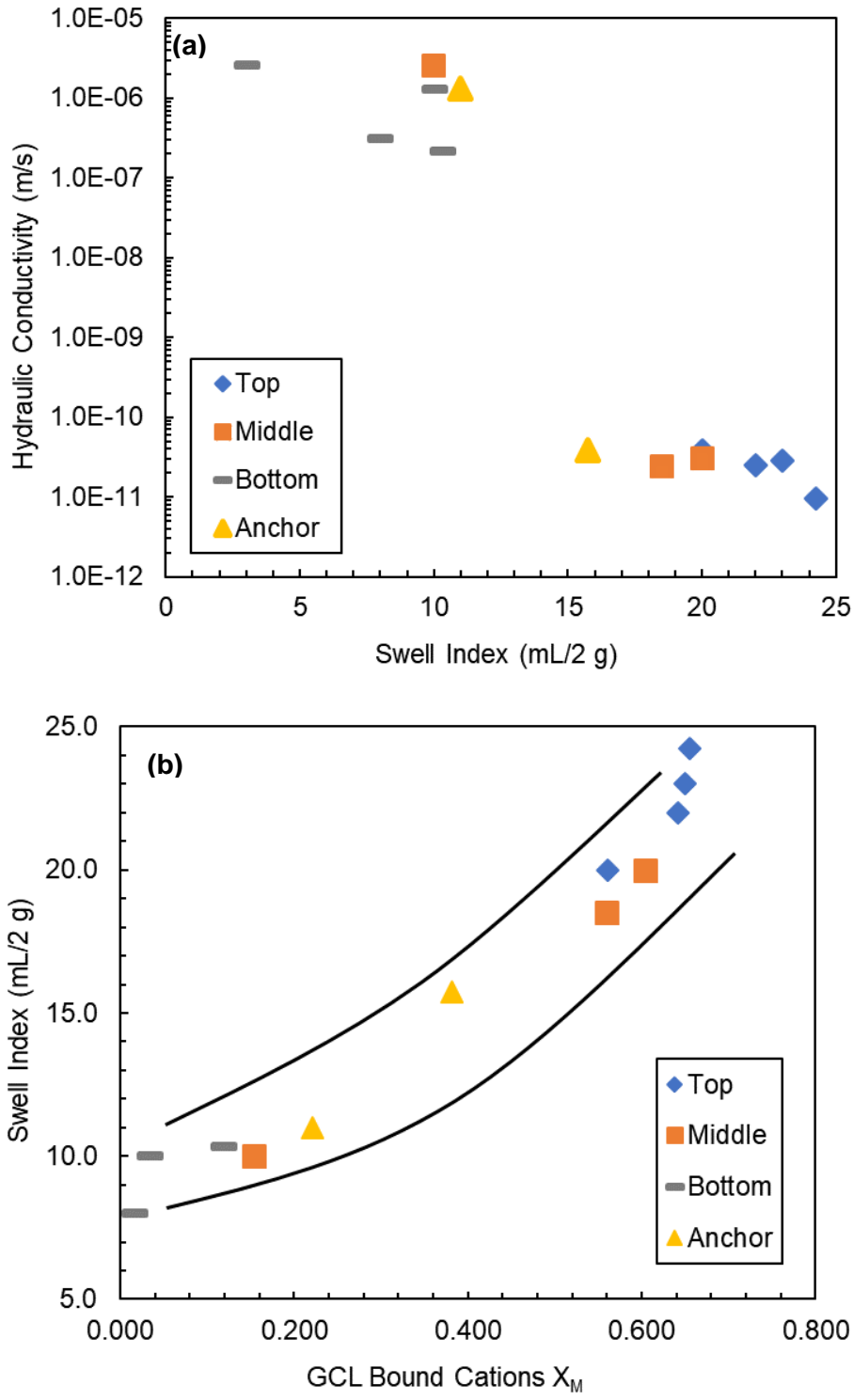


Fig. 3.7. Hydraulic conductivity of exhumed GCL versus swell index (a) and swell index versus the major bound cation monovalent mole fraction (X_M) of the exhumed bentonite (b).

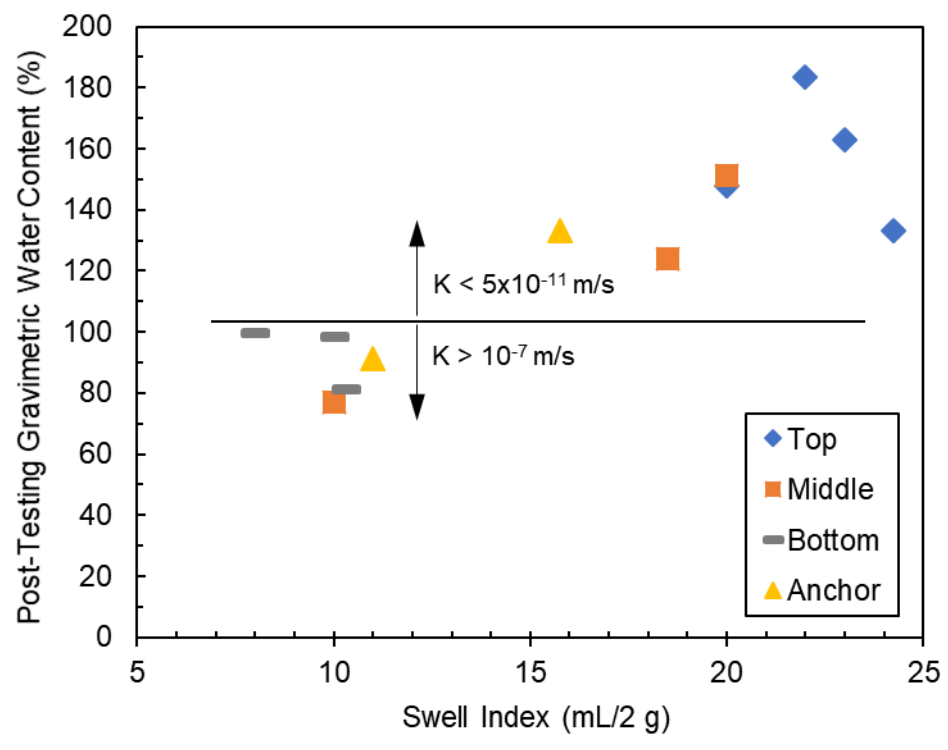


Fig. 3.8. The gravimetric water content of the exhumed GCL immediately following hydraulic conductivity testing with average water versus the swell index.

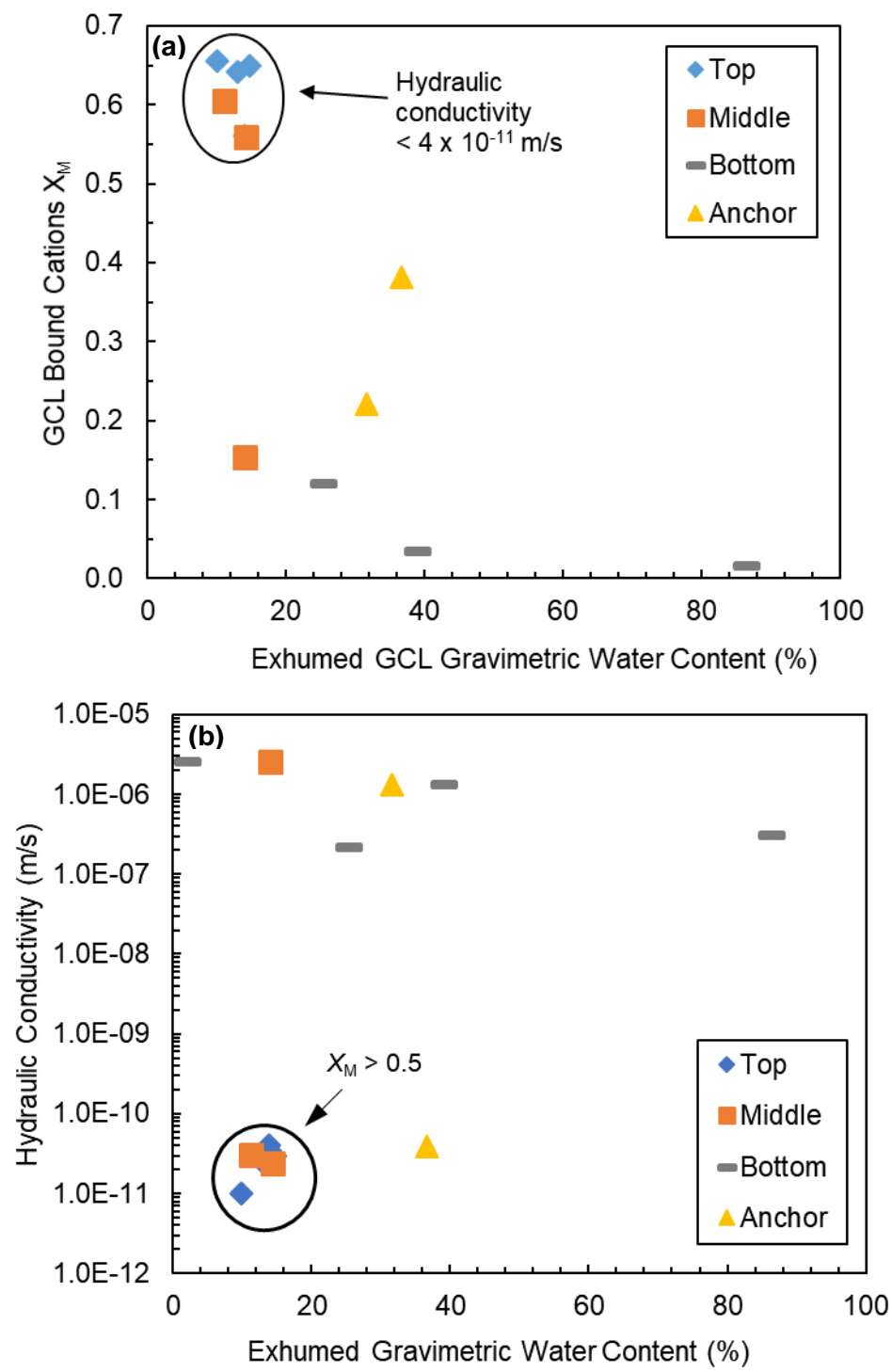


Fig. 3.9. The monovalent mole fraction of major bound cations on the exhumed GCL bentonite versus the exhumed GCL gravimetric water content (a) and hydraulic conductivity versus exhumed gravimetric water content of GCL (b).

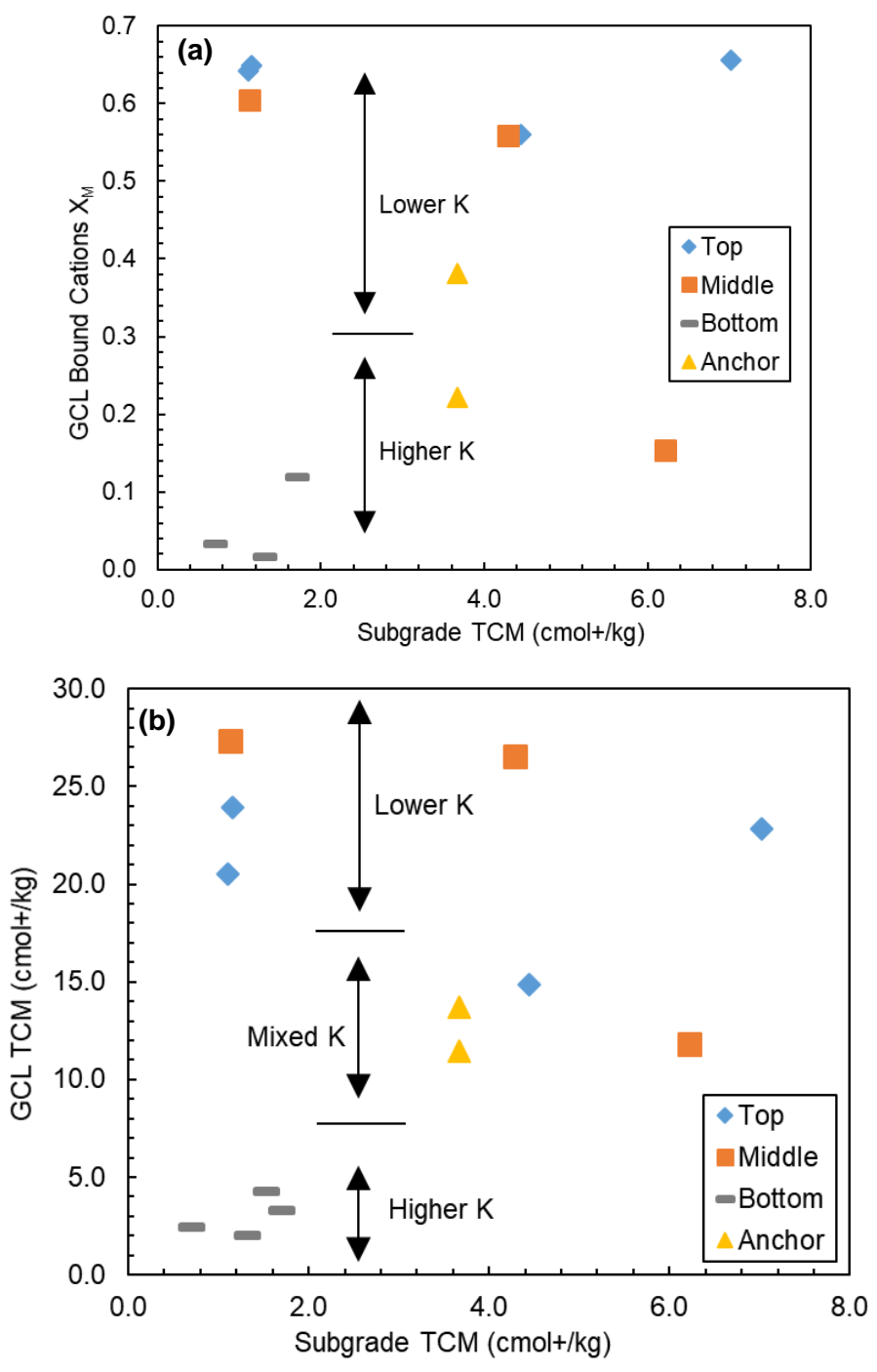


Fig. 3.10. The monovalent mole fraction of major bound cations on the exhumed GCL bentonite versus the subgrade total soluble cation charge per mass (TCM) (a) and the GCL TCM versus the subgrade TCM (b). GCL with higher K had $K > 10^{-7}$ m/s and GCL with lower K had $K < 4 \times 10^{-11}$ m/s.

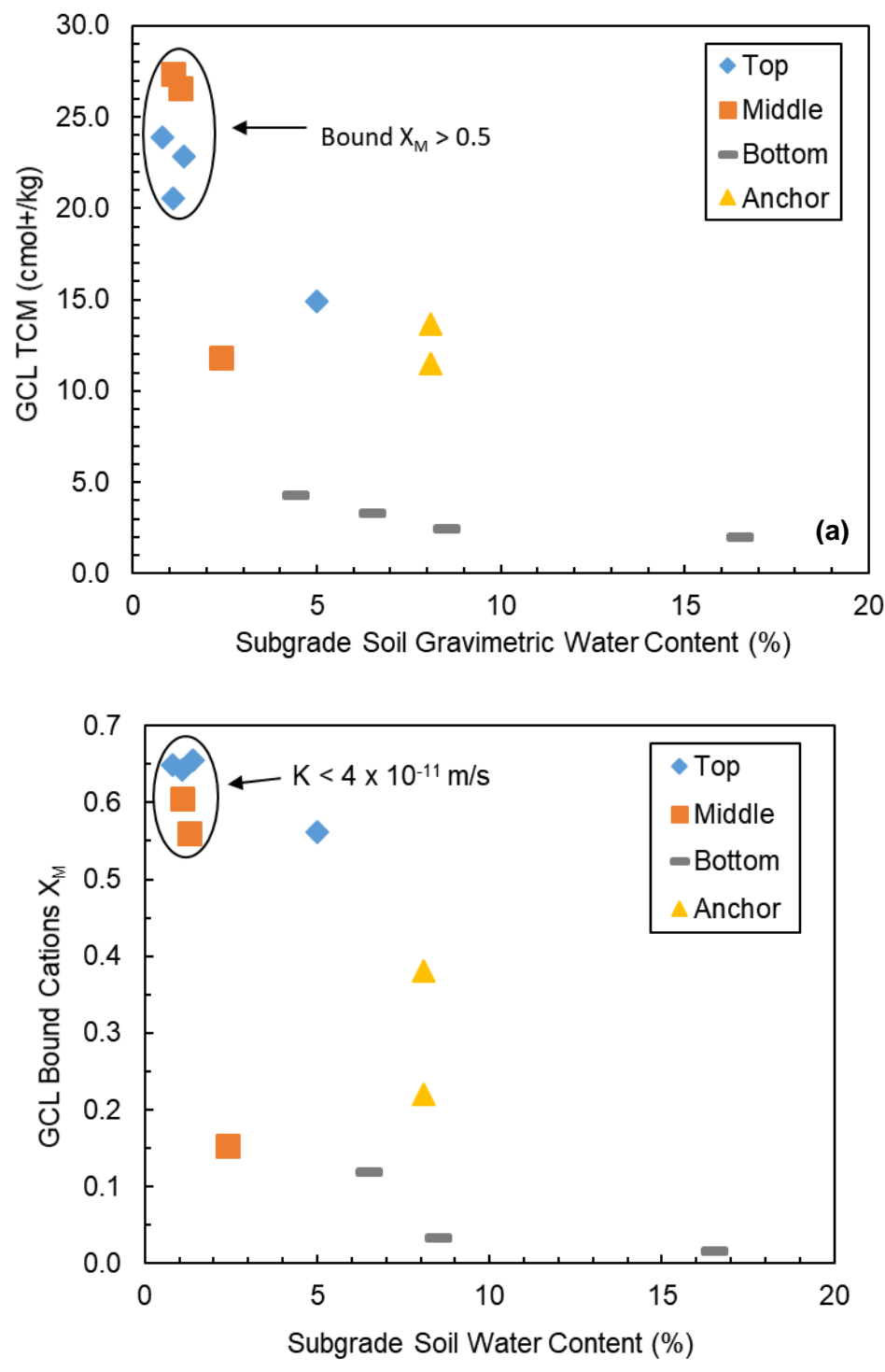


Fig. 3.11. The GCL total soluble cation charge per mass (TCM) versus the subgrade soil gravimetric water content (a) and the monovalent mole fraction of major bound cations on the exhumed GCL bentonite versus the subgrade soil water content.

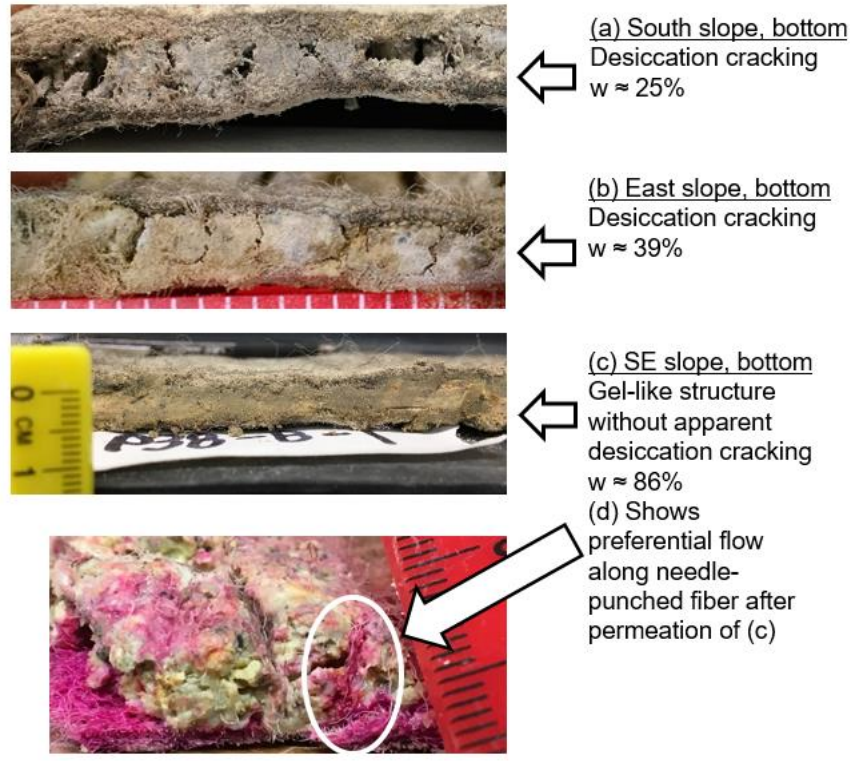


Fig. 3.12. Cross sections of GCL with hydraulic conductivity $>10^{-7}$ m/s and varying exhumed water contents. Image (d) shows specimen from (c) following permeation with rhodamine dye.

4 Observations of Bentonite Erosion in Composite Liner System Exposed to the Atmosphere for 12 Years

4.1 Abstract

The erosion effects of a 12-yr atmospheric exposure on a composite liner are analyzed herein. The composite liner consisted of black geomembrane (GM) overlying conventional sodium bentonite geosynthetic clay liner (GCL), and previous research shows that long-term atmospheric exposure of these geosynthetics may cause susceptibility to bentonite erosion induced by GM temperature cycling and down-slope moisture migration. Mass per unit area testing of GCL relative to position along the slope length showed some variance at top and mid-slope positions. Significant material accumulation and localized erosion was measured and observed near the slope bottom positions. Large amounts of eroded material, predominately consisting of bentonite, accumulated near the slope bottom above the GCL and below the GM. Observations of erosion rivulets at mid-slope locations and moisture contents measured near the slope bottom indicated that long-term down-slope moisture migration enabled bentonite erosion.

4.2 Introduction and Background

Composite liners consisting of geomembrane (GM) overlying geosynthetic clay liner (GCL) may effectively function as hydraulic barriers, but the performance of these liners is significantly dependent on quality control during installation and applying timely protective coverage following installation (Rowe 2012; Rowe et al. 2003, 2014; Take et al. 2015). For example, GM punctures during liner installation subsequently allow for leachate to rapidly encounter the underlying layers. Poor seam quality can compromise GM integrity, and improper placing of GCL overlaps may result in a weak point with high leakage potential. Quality control concerns are greatly heightened when a protective ballast layer is not installed above the composite liner in a timely manner. The lack of significant effective stress on uncovered liner systems increases GM wrinkling and allows

for greater shifting of liner materials. On sunny days, black GM is susceptible to severe temperature cycling induced by solar energy. The combination of GM temperature cycling and minimal effective stress enables severe erosion of bentonite in the underlying GCL.

Large scale field experiments at the Queen's University in Kingston, Canada established a mechanism for GCL erosion caused by long-term solar exposure of an uncovered GM over GCL lining system (Brachman et al. 2014; Rowe et al. 2016; Take et al. 2015). A composite liner consisting of a black 1.5 mm HDPE geomembrane overlying GCL was installed and left exposed for 4 years. The liner included a sloped (3H: 1V) section that was 21 m long by 76 m wide. The slope faced south to maximize solar radiation exposure. Evidence of erosion was first noted after 3.6 years of exposure when the overlying GM was cut in specific places to allow for observation of the underlying GCL. Discoloration in the form of downslope streaks suggested down-slope moisture migration and internal erosion of bentonite, which was confirmed by GCL exhumation and subsequent mass per area measurements. The lowest mass per unit area in an eroded area was 90 g/m^2 , whereas the mean mass per unit of new GCL was 3900 g/m^2 . A follow-up investigation showed that irrecoverable erosion effects occurred at around 12 months of exposure. The severe erosion of the GCL was attributed to daytime heating of the GM, which can reach upwards of 70°C , and subsequent nighttime cooling causing wrinkles induced by thermal cycles (Take et al. 2015). The air underneath wrinkles is partially insulated. During the day, the insulated air pockets may reach temperatures significantly higher than ambient resulting in significant evaporation from the underlying GCL. The geomembrane temperature may then drop below the insulated air temperature as solar radiation decreases in the evening. Overnight, condensation forms on the GM underside. Droplets then run down the underside of the GM until they reach a "drop off" point, such as a cross-slope wrinkle, or until they contact the underlying material. The result is a steady down-slope flow of distilled water that promotes erosion. The following observations show evidence of the same erosion process caused by the mechanism of geomembrane temperature cycling and down-slope moisture migration at a large field site in

California. The composite liner (black GM over conventional sodium-bentonite GCL) under consideration remained exposed for 12 years, and no protective layer was installed.

4.3 Exhumation and Testing Methods

GCL samples were obtained from a composite liner along the side slopes (2:1 slope, 26.6°) in an unused cell at a municipal solid waste landfill located in a temperate climate zone (Csb - temperate, dry summer, warm summer, Peel et al. (2007)) in California. Samples were exhumed from southern and eastern slopes near top of slope, mid-slope, and toe (bottom) of slope. Samples were also exhumed from the anchor trench (A1 and A2). A plan view of relative GCL exhumation locations is shown in Fig. 4.1, and GCL sample designations are shown in Table 4.1. The GCL was needle punched with nonwoven cover and carrier geotextiles and originally contained granular Na-bentonite. Additional specimens were exhumed from the composite liner from locations of bentonite accumulation (Table 4.2).

4.3.1 Mass per Unit Area

Mass per area measurements were conducted in accordance with ASTM D5993-14. Square specimens with 100 mm side length were cut from the exhumed GCL using a razor. The specimen perimeter was wetted to limit clay granule loss during cutting. One specimen was cut per GCL sample, and the resulting measurements of the whole GCL mass per unit area are listed in Table 4.1.

4.3.2 X-Ray Diffraction

X-ray diffraction was conducted by Mineralogy, Inc. (Tulsa, Oklahoma) using a method modified from Moore and Reynolds (1989) to determine the mineralogy of selected exhumed GCL and subgrade soil samples. Table 4.1 lists the montmorillonite fraction of select GCL samples. The preparation of XRD samples included grinding with a mortar and pestle, dispersion in dilute sodium phosphate solution using a sonic probe, vacuum-depositing on nylon membrane filters,

attachment to glass slides, and exposure to ethylene glycol vapor for 24 h. A Rigaku Ultima IV XRD system was used, and quantitative analysis employed the Rietveld method.

4.3.3 Swell Index

The swell index of the exhumed GCL contents was measured following ASTM 5890-11, using 2.0 g of oven dried and finely ground (passing #200 sieve) material. Deionized water was used as the testing reagent.

4.4 Observations of Erosion in Exposed Liner and Discussion

GCL samples were exhumed from locations near the slope tops, at mid-slope, near the slope toe/bottom, and from the anchor trench. Mass per unit area measurements relative to the exhumation position are shown in Fig. 4.2. The anchor trench was covered by about 0.3 m of soil, providing protection against GM temperature cycling and erosion. The anchor trench GCL may be considered as a control for comparison, with average mass per unit area of 5.3 kg/m². Relative to the anchor trench, the average mass per unit area of the top samples was lower. The top slope samples averaged 4.5 kg/m². The mid-slope samples showed a greater average (5.7 kg/m²) and greater variance relative to the top-slope samples. The high mass per unit area of two mid-slope samples (6.2 and 6.1 kg/m²) relative to the anchor trench is suspected to be attributable to on-going down-slope erosion, resulting in variable levels of accumulated material near mid-slope. Variance was greatest at the slope toe/bottom, where one GCL sample experienced nearly complete erosion of its internal contents. Elsewhere at the study site, significant amounts of material accumulated near the slope toe above the exhumed GCL and below the overlying geomembrane.

The top side of an exhumed GCL from a mid-slope location showed evidence of a down-slope erosion rivulet (Fig. 4.3), comparable to those identified in (Rowe et al. 2016). The thin (≈1-3 mm thick) layer of material appears to run down-slope in narrow paths. XRD analysis estimated the rivulet material to be 94% montmorillonite. Despite the rivulet presence, the exhumed GCL

mass per unit area was about average, indicating a lack of significant internal erosion. However, the mass per area of the sample was greater than that from the slope top by 0.4 kg/m^2 , suggesting that the slope-top may have experienced erosion. These observations agree with the findings from Rowe et al. (2016) which showed that bentonite streak locations did not directly correspond with internal bentonite erosion, but they were indicative of erosion occurring elsewhere. The rivulet marks a path of long-term down-slope moisture migration which enabled bentonite erosion. High exhumed moisture contents from slope toe locations are partially attributed to down-slope moisture migration resulting from the geomembrane temperature cycling. Multiple observations and specimens exhumed from near the slope toe showed accumulation of eroded material with elevated moisture contents.

A GCL sample exhumed from the bottom of the east slope had a layer of accumulated material $\approx 10 \text{ mm}$ thick on the top side of the GCL (Fig. 4.4). The material showed significant desiccation cracking, and tactile inspection suggests that the material was predominantly fines. Similar accumulation of bentonite near the slope toe was observed in (Rowe et al. 2016). XRD analysis, performed by Mineralogy, Inc (following a procedure modified from Moore and Reynolds (1989)), estimated the material composition as 85% montmorillonite. Swelling of the material was 5 mL/2 g , suggesting that multivalent cations were predominant in the montmorillonite exchange complex. The exhumed water content of the eroded material was 40%, which was large relative to most exhumed GCLs from the site. An additional specimen (“wedge”) of material was taken from a large area of material accumulation above the GCL near the bottom of the east slope. The wedge was up to 90 mm thick, and the material water content was relatively high (95%). The water content of the wedge shows that moisture accumulation coincided with eroded material accumulation. XRD testing estimated the MMT content at 73%, indicating that a large portion of the material was eroded bentonite. The SI was 5 mL/2 g , again suggesting significant multivalent cation exchange. Localized areas of severe internal erosion of the bentonite within the GCL was also observed near the slope toe.

The erosion of the contents of an exhumed GCL sample from the toe of the south slope (SS-B) is shown in Fig. 4.6. The measured mass per unit area of the eroded sample, 1.6 kg/m², mostly consisted of the geotextiles. The exhumed water content of the material remaining in the GCL was 2%, which was the smallest water content observed by 8% among the exhumed GCL, and the swell index was 3 mL/2 g. XRD analysis estimated the remaining material to be 57% montmorillonite, which was significantly lower than the average of the other selected GCL specimens (78%). The lack of remaining bentonite material in the GCL likely contributed to the very low water content (2%) at the time of exhumation, which is not believed to be representative of historical moisture availability.

4.5 Summary and Conclusions

Overall, the findings from the exhumed GCL study correspond with the erosion mechanisms detailed by Rowe et al. (2016). Significant down-slope moisture migration and bentonite erosion occurred during the 12 yr atmospheric exposure period, and accumulation of bentonite was observed near the slope bottom. Elsewhere near the slope bottom, nearly complete mass loss was observed from an exhumed GCL, demonstrating the localized effects that may occur as a consequence of erosion behavior. The erosion observed herein emphasizes the importance of quickly installing a protective cover layer over landfill composite liners.

4.6 REFERENCES

See end of document.

4.7 Erosion Observation Tables and Figures

Table 4.1. Properties of GCL exhumed from study site.

GCL Sample ID ^a	GCL Water Content (%)	Subgrade Water Content (%)	GCL Mass Per Area (kg/m ²) ^b	MMT ^c Content (%)	Swell Index (mL/2 g)
New GCL			4.4 ^d		24 ^d
ES-T	14	5.0	4.5	78	20
ES-M	14	2.4	6.2	75	10.0
ES-B	39	8.5	4.9	79	10.0
SS-T	13	1.1	4.4	NM	22.0
SS-M	11	1.1	6.1	NM	20.0
SS-B	2	4.4	1.6	57	3.0
SE-T	15	0.8	4.5	81	23.0
SE-M	14	1.3	4.8	73	18.5
SE-B	86	16	5.8	82	8.0
A1	32	8.1	5.4	78	11.0
A2	37	8.1	5.2	NM	16.0
PS-T	10	1.4	NM	NM	24.0
SS-B, Seam Overlap	25	6.5	NM	NM	10.5

^aES = east slope, SS = south slope, A = anchor trench, SE = southeast corner slope, T = top, M = middle, B = bottom, PS = panel separation; ^bincludes geotextiles and bentonite, initial mass per unit area of installed GCL ~ 5 kg/m²; ^cMMT = Montmorillonite. NM indicates not measured; ^dReported by manufacturer.

Table 4.2. Properties of additional erosion specimens.

Sample ID ^a	Specimen Water Content (%)	MMT ^b Content (%)	Quartz Content (%)	Feldspar Content (%)	Swell Index (mL/2 g)
New GCL					24 ^c
Wedge	95	73	6	14	5.0
ES-B Accumulation	40	85	4	8	5.0
SE-M Rivulet	NM	94	2	0	NM

^aES = east slope, SE = southeast corner slope, M = middle, B = bottom; ^bMMT = Montmorillonite. NM indicates not measured; ^cReported by manufacturer.

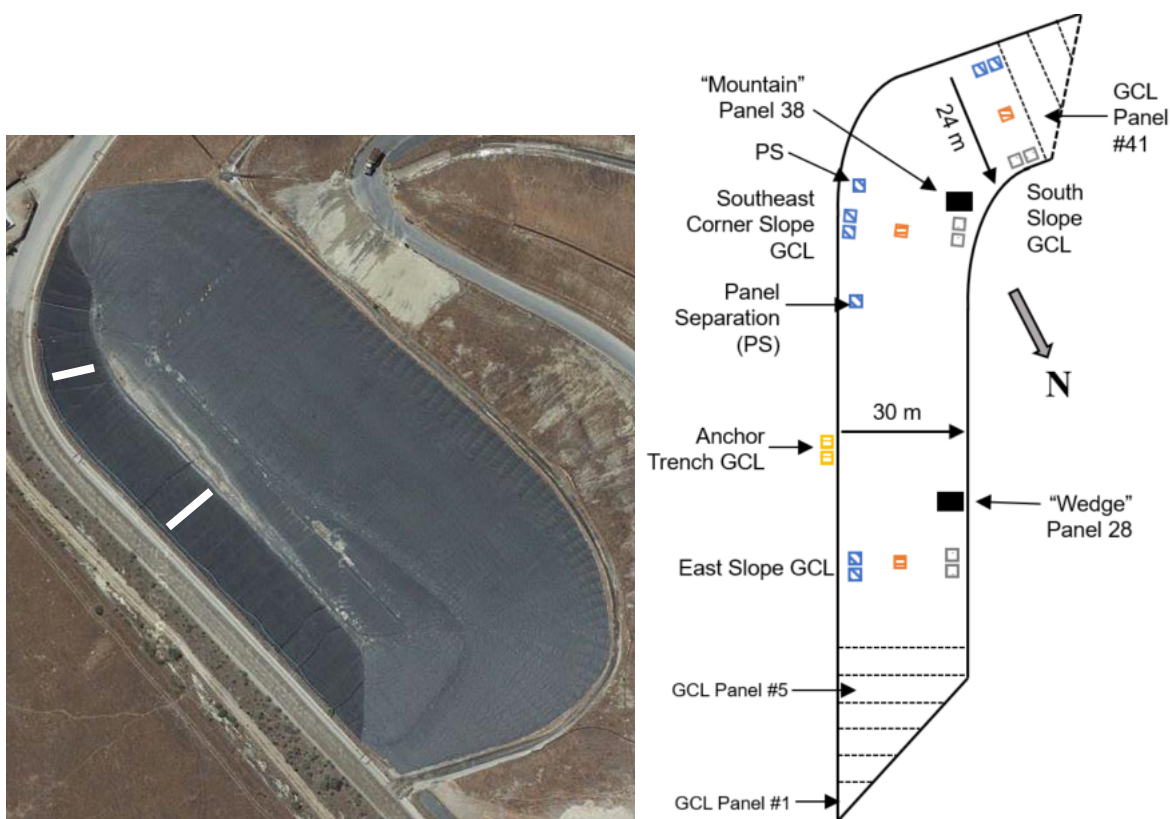


Fig. 4.1. Overhead aerial image of landfill site (left), courtesy of Professor Jim Hanson at Cal Poly San Luis Obispo. White lines indicate approximate exhumation locations of the east and southeast corner slopes. Plan view of landfill slope and locations of GCL sample exhumation. Image is not to scale. Colored squares indicate GCL exhumation positions. Color corresponds to location along slope (top=blue, middle=orange, bottom/toe=gray, anchor=yellow).

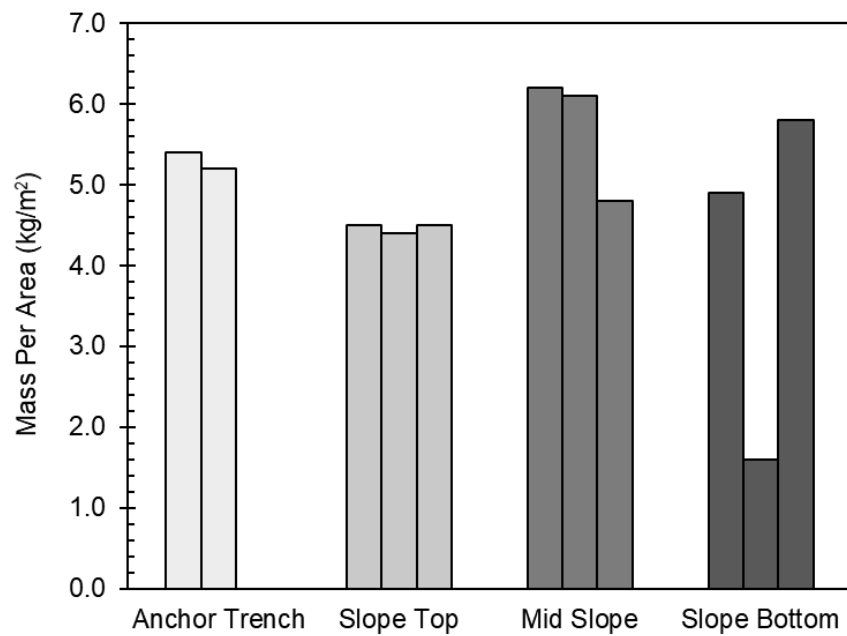


Fig. 4.2. Mass per area of whole GCL vs. location.



Fig. 4.3. Rivulets of eroded montmorillonite above GCL exhumed from the middle of the southeast corner slope (SE-M erosion rivulet).



Fig. 4.4. Accumulation of bentonite near the toe of the east slope. The accumulated material lies above the GCL and below the GM. Accumulated material was not included in the mass per unit area measurements.



Fig. 4.5. Area of widespread material accumulation near the bottom of the slope, referred to as the "wedge". Material gathered above the GCL and underneath the GM. Image courtesy of Professor Jim Hanson at Cal Poly San Luis Obispo.

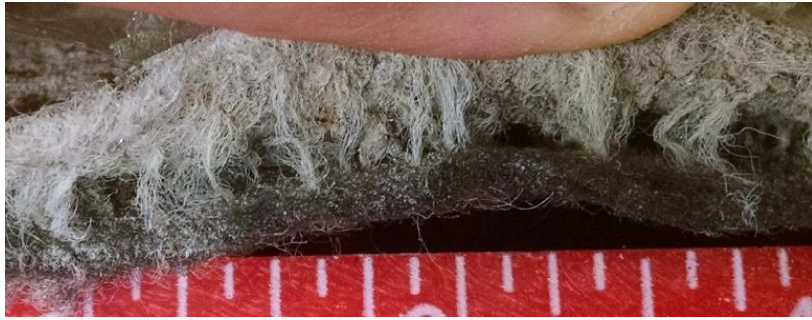


Fig. 4.6. Erosion of the internal contents of GCL exhumed from the bottom of the south slope

5 Challenges in Assessing the Polymer Loading of Bentonite Polymer Mixtures

5.1 Abstract

Bentonite-polymer mixtures may function as effective hydraulic barriers to leachates with extreme chemical properties, but their performance requires product uniformity to prevent the formation of preferential flow channels. Assessing the product uniformity requires an accurate and precise method for measuring the polymer content of the mixtures, but there is not an accepted standard method as of the time of writing. Loss on ignition testing has been used to estimate the polymer content, but varying test parameters and assumptions have been applied in the literature. Difficulties encountered during the polymer content estimation of a standardized product are detailed herein. Check tests were conducted to assess the accuracy and precision of a loss on ignition procedure for estimating the polymer content, and suggestions are made to standardize the polymer content estimation method. The very rapid rate of water vapor sorption by specimens of oven-dried polymer and bentonite was shown to cause significant error.

5.2 Introduction

Geosynthetic clay liners (GCLs) are composite materials that utilize a thin layer of highly swelling Na-bentonite to function as barriers to contaminant transport (Scalia et al. 2014; Shackelford et al. 2000). The montmorillonite (MMT) component of bentonite controls the swelling behavior. The swelling depends on the major cations in the MMT exchange complex and the chemistry of the hydrating solution (Benson and Meer 2009; Jo et al. 2001). Sodium is initially predominant in the MMT exchange complex of highly swelling Na-bentonite, but exchange of the original sodium for polyvalent cations in the hydrating solution results in significant loss of swelling potential and large increases in hydraulic conductivity (Jo et al. 2005; Kolstad et al. 2004a). Thus, the effectiveness of conventional GCLs as transport barriers is susceptible to polyvalent cation exchange in electrolyte solutions with significant polyvalent cation availability ($> \approx 5$ mM).

Researchers have modified conventional Na-bentonite GCLs through the addition of organic components to increase the GCL effectiveness in solutions with large electrolyte concentrations. Scalia et al. (2014) used polymerization of acrylic acid to form Na-polyacrylate in the interlayers of Na-bentonite. The resulting material, referred to as bentonite-polymer composite (BPC), maintained a hydraulic conductivity to 500 mM CaCl₂ approximately five orders of magnitude lower than for conventional Na-bentonite GCL (10^{-10} cm/s vs. 10^{-5} cm/s). The BPC also maintained relatively low hydraulic conductivity to 1 M solutions of HNO₃ and NaOH. The modified BPC GCLs show significant potential as hydraulic barriers, but the effectiveness of polymer-bentonite mixtures used as hydraulic barriers is partly dependent on the uniform distribution of polymer throughout the mixture. Additionally, polymer may elute from the GCL during hydraulic conductivity testing, and quantifying the degree of polymer elution requires accurately assessing the polymer loading.

Variance in polymer content may lead to local areas with preferential flow channels and high hydraulic conductivity. Accurately quantifying the uniformity of polymer loading requires a standardized procedure to obtain representative specimens from the GCL and to accurately assess the polymer content. Loss on ignition (LOI) testing is typically used to measure polymer content, but a standard method for polymer-bentonite mixtures is not codified and assumptions may vary between studies (Scalia et al. 2014; Tian et al. 2017). Important considerations include the process of specimen extraction from the GCL without disrupting the initial polymer content, determination of a sieve requirement to standardize specimen size, and the time and temperature settings used during LOI. As of the time of writing, the author is unaware of a standard industry-accepted methodology for assessing the polymer loading of polymer-bentonite mixtures. This paper details challenges and observations noted during the laboratory assessment of polymer loading of a bentonite-polymer GCL product. Polymer loading assessments varied over a 1.5% range between multiple operators, which is not satisfactory. Recommendations are provided

concerning specimen handling and LOI procedure to improve testing standardization and reproducibility.

5.3 Background

ASTM D7348 has been referred to for LOI testing of bentonite-polymer mixtures, but the test procedure is intended for solid combustion residues and some specifications are inappropriate for bentonite polymer mixtures (Akin et al. 2017; Tian et al. 2017). ASTM D7348 specifies pulverizing of samples to pass a No. 60 sieve, but observations during polymer loading assessments suggest that polymer loss as dust would occur if bentonite-polymer specimens were pulverized. The specified temperatures are higher than necessary for igniting polyacrylate, and the result calculations do not attempt to distinguish between different combustible components of the original samples. The holding period at maximum temperature is not specified explicitly.

Assumptions concerning the extent of polymer combustion and the mass loss experienced by bentonite will affect polymer loading assessments (Scalia et al. 2014; Tian et al. 2017). The general procedure for LOI testing of polymer loading followed in previous studies includes grinding to pass a specified sieve size, oven-drying of the specimen between 105-110°C, ignition at 550°C for ≈ 4 h, and cooling in a desiccator followed by mass measurements. One approach accounts for impartial combustion of the polymer and structural water loss from the bentonite during the 550°C ignition by separately igniting polymer and bentonite specimens (Akin et al. 2017; Scalia et al. 2014; Scalia and Benson 2016). Scalia et al. (2014) found that a sample of bentonite lost $1.6 \pm 0.1\%$ mass on ignition (corresponding to removal of structural water) and a polymer sample (polyacrylate) lost $74.7 \pm 0.0\%$ mass on ignition (10 replicate tests). The polymer loading of bentonite-polymer mixtures was then assessed by applying the assumption that bentonite would lose 1.6% mass on ignition and polymer would lose 74.7% mass on ignition in the combined specimens. The assumption of complete polymer combustion has been applied in other studies.

5.4 Materials and Methods

Initial testing was conducted on a commercially available bentonite-polymer GCL. Specimens for testing (squares with ≈ 50 mm side length) were cut from the GCL sample product using utility scissors. The contents were then removed from the specimens, ground to pass through a No. 10 sieve, and used for testing. Separate batch samples of sodium-bentonite and polymer from the GCL were also supplied. The composition of the polymer is proprietary.

Loss on Ignition Procedure: The loss on ignition was conducted at 550°C for 4 hr using a gradual warm-up period. Following the 4 hr ignition period, the furnace was set to gradually cool to 110°C and hold 110°C until the specimens were removed. Specimens of the bentonite-polymer mixture used for testing averaged 5 g mass. The LOI parameter is defined as:

$$LOI = \left(\frac{M_i - M_f}{M_i} \right) \times 100\% \quad (5.1)$$

where M_i is the initial dry mass of the specimen and M_f is the final specimen mass after ignition at 550°C . LOI testing is used herein to refer to the 4 hr ignition period at 550°C .

Polymer Loading Estimation from LOI: During the ignition period of an LOI test, the polymer will partially combust, and the bentonite will lose structural water (Scalia et al. 2014). Thus, measurement of LOI does not directly reflect the actual polymer loading. The polymer loading is defined as:

$$\text{Polymer Loading} = \frac{M_p}{M_i} \quad (5.2)$$

where M_p is the initial dry mass of the polymer in the specimen and M_i is the initial dry mass of the entire specimen. Calculating the polymer loading requires estimating the initial polymer mass in the test specimen. The initial and final masses measured during the loss on ignition test may be used to estimate the polymer loading of the original sample. Starting with the measured values

of M_i and M_f , the initial dry specimen mass and the post-LOI mass, respectively, the following equations may be written:

$$M_i = M_B + M_P \quad (5.3)$$

$$M_f = \beta M_B + \rho M_P \quad (5.4)$$

where M_B and M_P are the mass of dry bentonite and polymer, respectively, in the initial specimen before LOI testing, and β and ρ are the fractions of dry bentonite and polymer, respectively, retained after LOI testing. These equations assume that the initial specimen only consists of a dry raw-bentonite portion and a dry polymer portion, with the respective masses indicated by M_B and M_P . From these two above equations, an equation for the polymer loading may be written in terms of the experimentally measured values (M_i and M_f) along with β and ρ , where β and ρ are determined through separate experiments. The polymer loading of a sample may be estimated using experimentally derived values:

$$\frac{M_P}{M_i} = \frac{M_f - \beta M_i}{M_i(\rho - \beta)} \quad (5.5)$$

The results from attempts to estimate the polymer loading of the bentonite-polymer GCL product are shown in Table 5.1. Following the challenges encountered during the product polymer loading assessment, a method was devised to assess the reproducibility of the LOI method.

Bentonite-polymer mixture specimens, referred to as check specimens, were prepared with known masses of polymer and bentonite to assess LOI reproducibility. Two different methods were used to prepare the check specimens: oven-dry preparation and air-dry preparation. Specimens prepared using the oven-dry method were oven dried in large batches at 110°C until constant mass was achieved. The specimens were then removed from the oven and immediately distributed into crucibles for LOI testing. Specimens prepared using the air-drying method were taken from sample batch containers which were air dried to constant mass in the laboratory

environment. The initial dry mass of the air-dried specimens was calculated using known air-dry water contents of the batch container samples. The results from the check specimens are shown in Table 5.2.

5.5 Findings and Discussion

The estimations of polymer loading using measurements from 4 LOI test operators are shown in Fig. 5.1. The range of polymer loading estimates was 1.5%, and the largest range for an individual operator was 0.8%. The variance may be attributable to several factors, complicating the analysis of results. The method of specimen extraction from the bentonite-polymer GCL was not fully standardized. The area of the GCL product from which the specimens were extracted also influences the representativeness of the specimen polymer loading relative to the sample polymer loading. Specimens removed from the edge of a GCL sample may differ in polymer loading due to contents falling from the GCL sample during handling. The procedure used when conducting the LOI test, such as the selection of specimen mass and the method of determining the dry mass, may affect the loading assessment. The check specimen tests were specifically conducted to assess the LOI test procedure accuracy and reproducibility. Additional research is needed to understand the effects of specimen extraction and preparation procedures.

Specimens with known dry mass of polymer and bentonite were prepared to assess the accuracy of the polymer loading estimation. Batches of polymer and bentonite were oven-dried to 110°C until constant mass was achieved. Check specimens were then prepared by adding the oven-dried material to crucibles to achieve the polymer loadings in Table 5.2. Following LOI testing, the specimens were kept at 110°C until the operator was ready to weigh the specimens. The specimens were weighed immediately upon removal from the drying oven by placing an insulating material on the scale. The estimates of polymer loading following LOI testing are shown in Fig. 5.2. The estimates of polymer loading were, on average, 1.0% greater than the measured

polymer loadings, and the largest discrepancy was 1.5%. The results suggest that the testing procedure introduced a systematic bias. It was suspected that water vapor sorption occurring during the handling of oven-dry material caused the estimations of polymer loading to exceed the measured values.

The rate and magnitude of water vapor sorption by the oven-dry bentonite and polymer was assessed in the laboratory environment. Bentonite specimens averaging 5 g and polymer specimens averaging 0.4 g were oven-dried to constant mass and then exposed in the laboratory environment (three replicates each). The resulting increase in specimen masses due to water vapor sorption are shown in Fig. 5.3. Within 200 s of exposure the polymer mass increased by about 1.5% and the bentonite mass increased by about 0.25%. Water vapor sorption occurring upon specimen removal from a drying oven and before weighing will thus disrupt the accurate estimation of polymer loading by causing an overestimation of the oven-dry mass. The sorbed water mass during this time interval will inflate the LOI measurement, resulting in the systematic bias shown in Fig. 5.2.

The air-drying sample preparation method was used to reduce the influence of water vapor sorption on the polymer loading estimation. Check specimens were prepared from air-dried batch containers with known water contents. Fig. 5.4. shows the resulting estimations of polymer loading following the LOI procedure for 2 g and 5 g specimen masses. The agreement between the estimated polymer loading and the calculated polymer loading is greatly improved relative to the oven drying procedure. The 5 g specimens yielded the most accurate estimations with the largest discrepancy being 0.07%. The 2 g specimen showed larger discrepancies (up to 0.44%), but the accuracy was still improved relative to the oven-drying method.

5.6 Suggestions for Future Research

Accurately assessing the polymer loading of bentonite-polymer mixtures presents significant challenges. A comprehensive procedure is not proposed within, but recommendations

are made for future research. The results of this investigation suggest that an air-drying method may be preferable to assess the polymer loading of a bentonite-polymer GCL before and after hydraulic conductivity testing. The author suggests that, after hydraulic conductivity testing, a large representative specimen should be removed from the GCL and allowed to air-dry until the specimen may be readily ground to pass a #10 sieve. The specimen should then be thoroughly mixed and allowed to air-dry to constant mass in an atmosphere with controlled humidity. Material should then be taken to assess the air-dry water content and to conduct LOI testing. Additional general suggestions are as follows:

1. Operators must be aware and mindful of the rapid rate of water vapor sorption when handling dried bentonite-polymer specimens. Multiple measurements of the dry mass of specimens conducted over time should be used to ensure that a consistent dry mass has been achieved.
2. Using air-dried material reduces the error introduced by water vapor sorption and may be helpful when handling GCL specimens.
3. It is advisable to position the weighing scale as near to the drying oven as feasible.
4. Operators should strive to reduce specimen disturbance when extracting the contents of GCL. The grinding procedure should be carefully monitored to avoid losing polymer or bentonite as dust.
5. An insulating material may be placed on the weighing scale to allow for the immediate weighing of oven dried (110°C) specimens. The time required to transfer multiple oven dried specimens in and out of a desiccator for cooling to room temperature may allow for significant water vapor sorption to occur.

5.7 References

See end of document.

5.8 Tables and Figures

Table 5.1. Polymer loading measurements (%) during initial testing

Operator ID	Number of Replicates	Trial 1	Trial 2	Trial 3	Trial 4	Trial 5	Mean	Standard Deviation
A	5	3.7	3.3	3.6	3.3	3.5	3.5	0.18
B	3	3.0	3.5	3.0			3.2	0.29
C	3	3.7	4.2	4.5			4.1	0.40
D	4	3.0	3.6	3.0	3.2		3.2	0.28

Table 5.2. Results of LOI testing of the check specimens using the oven-dry preparation method or the air-dry preparation method.

Oven-Dry Method (≈5g specimen size)		Air-Dry Method (≈2g and ≈5g specimen size)			
Polymer Loading from Measured Oven-Dry Mass (%)	Estimation of Polymer Loading following LOI (%)	Polymer Loading from Air-dry batch water contents (%)	Estimation of Polymer Loading following LOI (%)	Polymer Loading from Air-dry batch water contents (%)	Estimation of Polymer Loading following LOI (%)
1.0	1.56	0.99	1.43	1.01	1.00
2.5	3.28	2.50	2.79	2.50	2.46
5.0	5.84	5.00	5.17	4.99	4.95
7.5	8.95	7.50	7.77	7.51	7.55
10.0	11.53	9.98	10.19	9.98	10.05

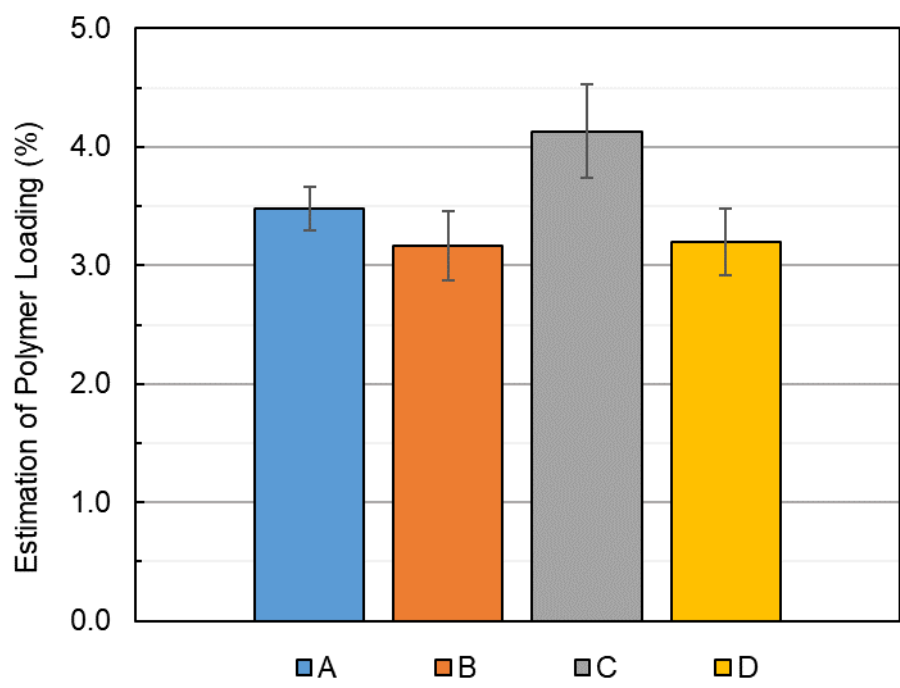


Fig. 5.1. Polymer loading measurements for commercial bentonite-polymer mixture from four operators.

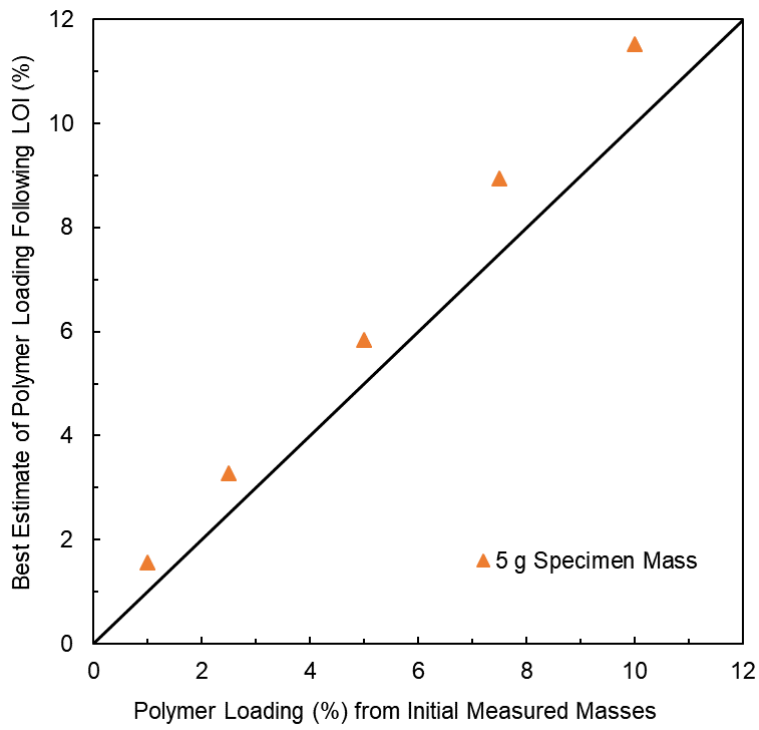


Fig. 5.2. Comparison of the best estimation of polymer loading following LOI testing vs. the polymer loading based on the initial measured masses of bentonite and polymer. The specimens were prepared by measuring out dried polymer and bentonite under atmospheric conditions.

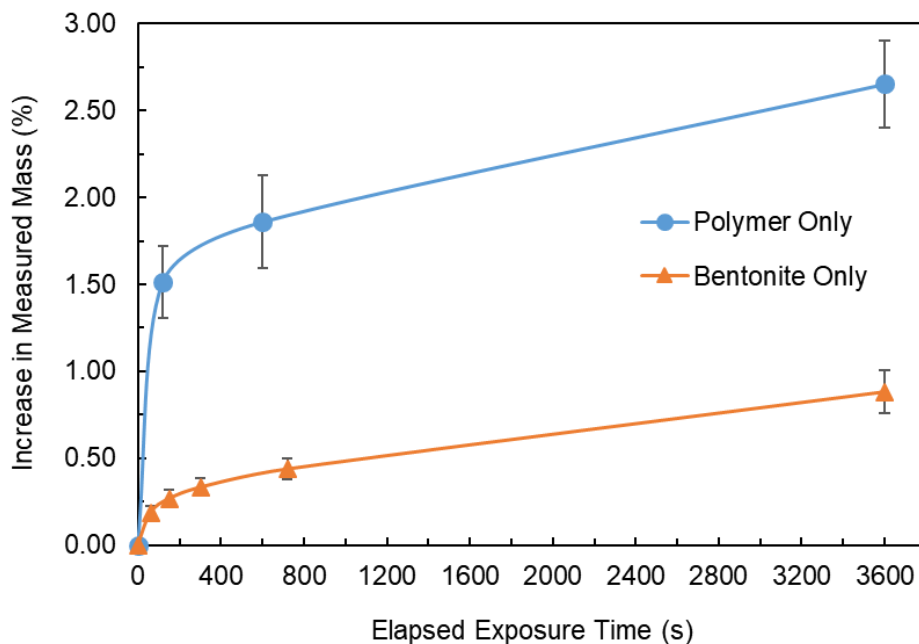


Fig. 5.3. Increase in mass of oven-dried (110°C) bentonite-polymer mixture as a function of time since removal from the oven. Sample exposed to atmosphere in laboratory, and three replicate tests were conducted.

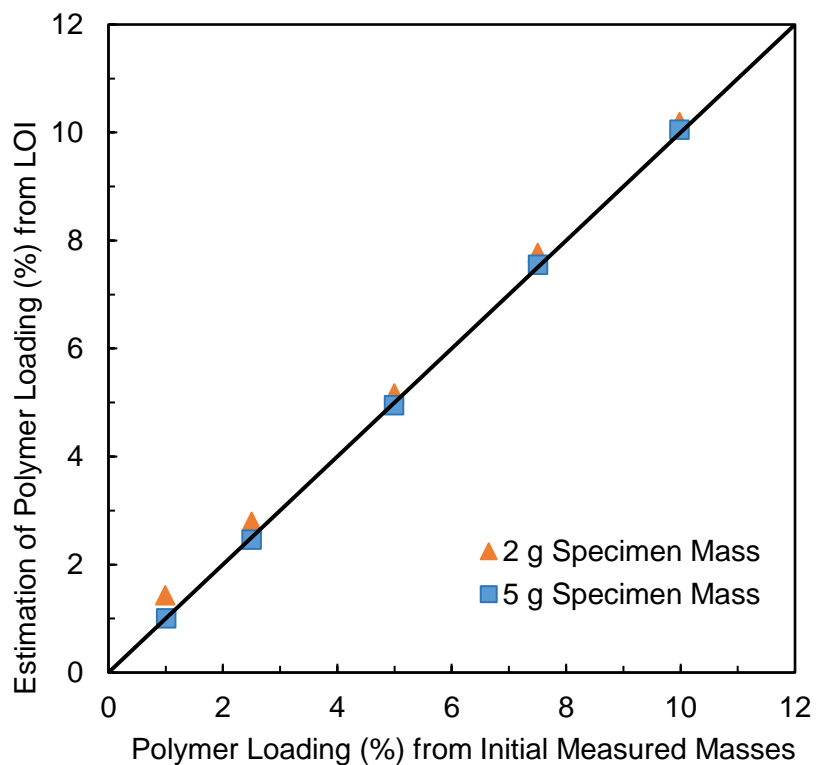


Fig. 5.4. Estimation of polymer loading using air-dried specimen preparation method. Known air-dry batch water contents of the bentonite and polymer were used to calculate the actual polymer loading from initial measured masses.

6 Appendix

6.1 Composite Liner Exposure: Regulatory Applicability of Findings

Federal regulation of municipal solid waste was established under Subtitle D of the Resource Conservation and Recovery Act (RCRA). The United States Environmental Protection Agency (EPA) has the authority to develop and implement waste management requirements to achieve the goals of the RCRA. The EPA has set minimum national standards for municipal solid waste landfills, but individual states frequently implement more stringent standards and specifications. Current federal regulation at the time of writing (C.F.R., Title 40, Part 258 and 264) does not specify any explicit time requirement for the protective covering of the bottom liner system between the time of liner construction and the start of landfill operation for hazardous nor non-hazardous waste landfills. However, GCL manufacturers typically recommend the addition of protective covering within one month of liner installation, and individual states may establish time requirements for protective coverage. For example, Virginia Administrative Code (9VAC20-81-130) requires that, for a liner system consisting of geomembrane overlying GCL, any exposure period longer than 2 months will require "... a discussion of the adequacy of the GCL overlap". Virginia's requirement is more explicit than the federal regulations, but it does not address the possibility of the erosion and degradation (through unfavorable cation exchange) of the bentonite within the GCL.

A specific time requirement for the protective covering of a composite liner (GM over GCL) may be beneficial to ensuring the liner integrity, but the dependence of erosion on several factors should be considered. Geomembrane color, the use of powdered bentonite or a bentonite-polymer composite, or the presence of an up-facing polypropylene coating may work to prevent or slow the onset of erosion and bentonite degradation (Rowe et al. 2016). Efficient regulation would match protective cover requirements to the choice of liner material. The results of the exposure study herein indicate that more stringent coverage requirements are advisable for the

typical case of black geomembrane overlying conventional sodium-bentonite GCL. The extended duration of the atmospheric exposure herein is considered highly unusual. Still, investigations have shown that erosion may be expected within six months of exposure for black GM overlying conventional GCL (Rowe et al. 2016). More investigation may help to build confidence in the estimation of erosion onset. For the time being, formal regulation following manufacturer guidelines regarding liner protection is encouraged.

6.2 Exposed Liner Project – Additional Testing

To check the effect of permeant water and wet-dry cycling on hydraulic conductivity, samples A1 and A2 were selected for additional testing. These samples were selected because A1 had the largest swell index (11 mL/2 g) and bound cation X_M for samples with large hydraulic conductivities ($>10^{-7}$ m/s), and A2 had the lowest swell index (16 mL/2 g) and bound cation X_M for samples with small hydraulic conductivities ($<5 \times 10^{-7}$ m/s). A specimen was taken from sample A1 for hydraulic conductivity testing with deionized water to see if the more dilute solution would influence the hydraulic conductivity, and the results are shown in Fig. A.6.1. Upon the start of permeation, sample A1 had a hydraulic conductivity to deionized (DI) water approximately one order of magnitude less than that for the average water solution. However, the hydraulic conductivity gradually increased during the test duration, and the final hydraulic conductivity (9.4×10^{-7} m/s) with DI water was comparable to that with average water (1.2×10^{-6} m/s). Multivalent cation exchange with soluble cations (TCM = 13.7 cmol+/kg) originally on the specimen may have contributed to the increasing hydraulic conductivity.

Sample A2 was selected to test for susceptibility to wet-dry cycling effects due to its relatively low swell index amongst the samples with low hydraulic conductivities. A specimen was taken from sample A2 and oven-dried to constant mass. Oven-drying removes the bound water from the bentonite interlayer. To maintain a low hydraulic conductivity, the specimen would need to swell sufficiently to replace the lost bound water and form a gel-like structure.

Upon initial permeation, the oven-dried specimen experienced gradually decreasing hydraulic conductivity until becoming steady at 3.7×10^{-11} m/s (Fig. A.6.2). The specimen was removed from the permeameter at a cumulative inflow of 140 mL and allowed to air-dry to constant mass. On resuming the hydraulic conductivity testing, the specimen maintained a hydraulic conductivity even lower than for the first cycle (1.6×10^{-11} m/s). The specimen was again oven-dried, but sidewall leakage occurred on resumption of the hydraulic conductivity testing. Still, the initial results from two cycles of drying suggest that sample A2 had considerable resistance to wet-dry cycling effects.

6.3 Additional Figures and Tables

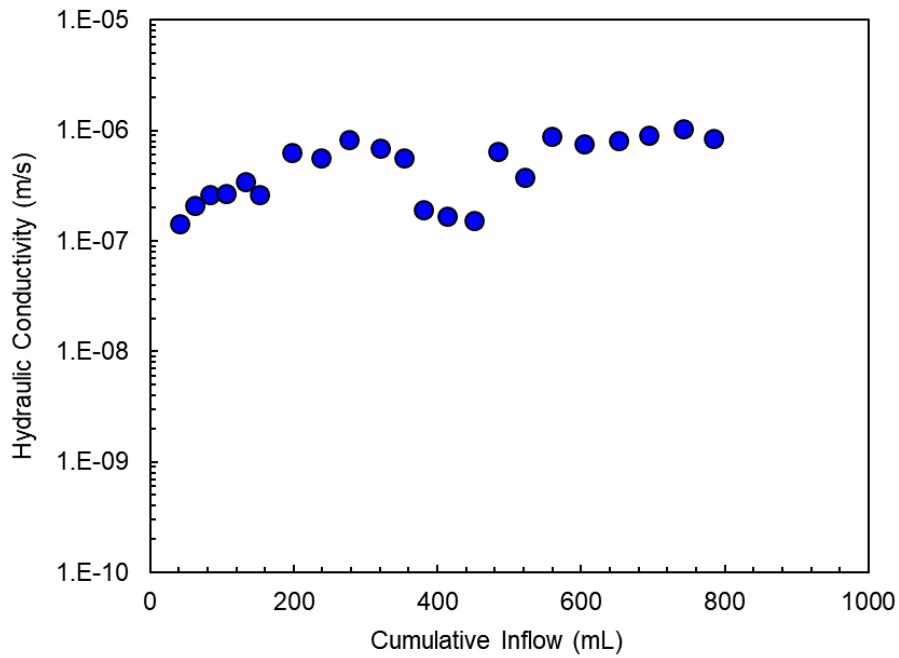


Fig. A.6.1. Hydraulic conductivity of sample A1 with deionized water versus the cumulative inflow volume.

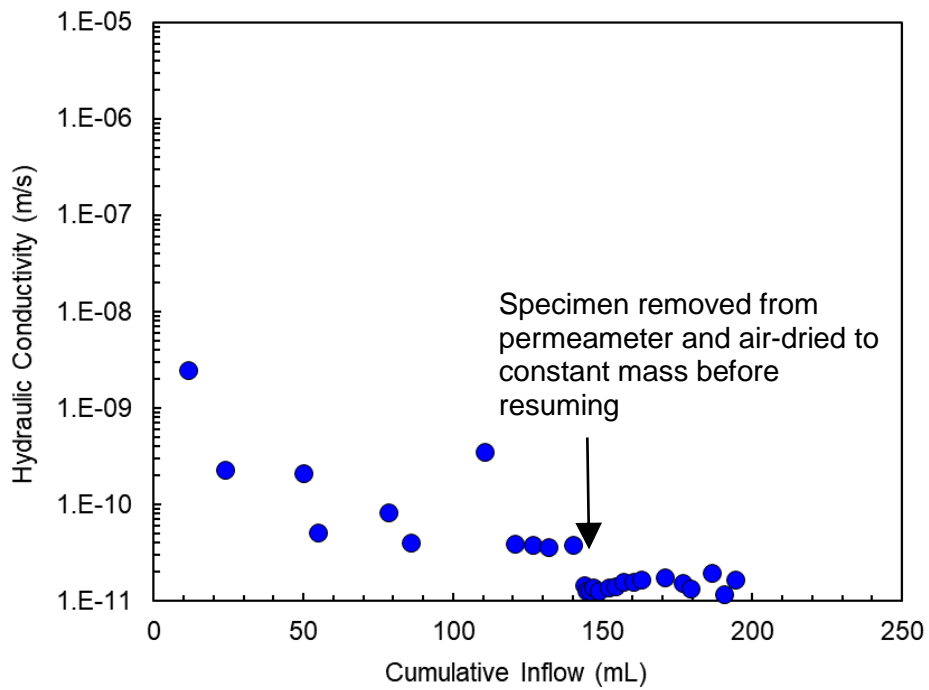


Fig. A.6.2. Hydraulic conductivity of sample A2 during wet-dry cycling tests with average water versus the cumulative inflow volume.

Table A.6.1. Exhumed GCL Exchange Complex – Soluble Cations

GCL Sample ID ^a	Soluble Cations TCM (cmol+/kg)	Na+ mole fraction	K+ mole fraction	Ca ²⁺ mole fraction	Mg ²⁺ mole fraction
New GCL	31.8	0.97	0.01	0.02	0.00
ES-T	14.9	0.95	0.02	0.02	0.01
ES-M	11.8	0.90	0.02	0.06	0.03
ES-B	2.4	0.52	0.17	0.21	0.10
SS-T	20.5	0.89	0.01	0.04	0.06
SS-M	27.3	0.84	0.01	0.06	0.09
SS-B	4.3	0.52	0.14	0.17	0.18
SE-T	23.9	0.83	0.01	0.07	0.09
SE-M	26.6	0.94	0.02	0.02	0.02
SE-B	2.0	0.26	0.17	0.36	0.20
A1	13.7	0.60	0.01	0.37	0.02
A2	11.5	0.78	0.04	0.11	0.06
PS-T	22.8	0.97	0.01	0.01	0.01
SS-B, Seam Overlap	3.3	0.84	0.10	0.04	0.02

^aES = east slope, SS = south slope, A = anchor trench, SE = southeast corner slope, T = top, M = middle, B = bottom, PS = panel separation; NM indicates not measured;

Table A.6.2. Exhumed GCL Exchange Complex – Major bound cation mole fractions

GCL Sample ID ^a	Cation Exchange Capacity (cmol+/kg)	Na+ mole fraction	K+ mole fraction	Ca ²⁺ mole fraction	Mg ²⁺ mole fraction
New GCL	31.8	0.97	0.01	0.02	0.00
ES-T	72.9	0.55	0.01	0.24	0.20
ES-M	70.4	0.14	0.01	0.41	0.39
ES-B	78.2	0.02	0.02	0.48	0.33
SS-T	79.8	0.63	0.02	0.14	0.12
SS-M	77.1	0.59	0.02	0.21	0.14
SS-B	NM	NM	NM	NM	NM
SE-T	76.6	0.64	0.01	0.18	0.11
SE-M	79.8	0.55	0.01	0.19	0.18
SE-B	72.9	0.00	0.01	0.45	0.22
A1	71.9	0.21	0.01	0.32	0.45
A2	73.4	0.37	0.01	0.28	0.25
PS-T	80.4	0.64	0.01	0.16	0.13
SS-B, Seam Overlap	73.9	0.09	0.03	0.41	0.34

^aES = east slope, SS = south slope, A = anchor trench, SE = southeast corner slope, T = top, M = middle, B = bottom, PS = panel separation; NM indicates not measured;

Table A.6.3. Subgrade Soil – Soluble Cations

Subgrade Soil Sample ID ^a	Soluble Cations TCM (cmol+/kg)	Na+ mole fraction	K+ mole fraction	Ca ²⁺ mole fraction	Mg ²⁺ mole fraction
ES-T	4.45	0.80	0.06	0.06	0.08
ES-M	6.22	0.68	0.01	0.18	0.13
ES-B	0.7	0.34	0.13	0.36	0.17
SS-T	1.11	0.60	0.37	0.00	0.04
SS-M	1.13	0.78	0.09	0.09	0.04
SS-B	1.53	0.58	0.25	0.10	0.08
SE-T	1.15	0.62	0.04	0.16	0.18
SE-M	4.29	0.44	0.10	0.24	0.22
SE-B	1.31	0.13	0.69	0.12	0.06
A1 ^b	3.67	0.13	0.52	0.18	0.17
A2 ^b	3.67	0.13	0.52	0.18	0.17
PS-T	7.02	0.22	0.63	0.08	0.07
SS-B, Seam Overlap	1.7	0.72	0.12	0.12	0.04

^aES = east slope, SS = south slope, A = anchor trench, SE = southeast corner slope, T = top, M = middle, B = bottom, PS = panel separation; NM indicates not measured; ^b1 subgrade soil sample from anchor

References

- Akin, I. D., Chen, J., Likos, W. J., and Benson, C. H. (2017). "Water Vapor Sorption of Bentonite-Polymer Mixtures Contacted with Aggressive Leachates." *Geotechnical Frontiers 2017: Waste Containment, Barriers, Remediation, and Sustainable Geoengineering (GSP 276)*, T. Brandon and R. Valentine, eds., Orlando, 209–219.
- Azad, F. M., Rowe, R. K., El-Zein, A., and Airey, D. W. (2011). "Laboratory investigation of thermally induced desiccation of GCLs in double composite liner systems." *Geotextiles and Geomembranes*, Elsevier Ltd, 29(6), 534–543.
- Benson, C. H., Kucukkirca, I. E., and Scalia, J. (2010). "Properties of geosynthetics exhumed from a final cover at a solid waste landfill." *Geotextiles and Geomembranes*, Elsevier Ltd, 28(6), 536–546.
- Benson, C. H., and Meer, S. R. (2009). "Relative Abundance of Monovalent and Divalent Cations and the Impact of Desiccation on Geosynthetic Clay Liners." *Journal of Geotechnical and Geoenvironmental Engineering*, 135(3), 349–358.
- Benson, C. H., Thorstad, P. A., Jo, H.-Y., and Rock, S. A. (2007). "Hydraulic Performance of Geosynthetic Clay Liners in a Landfill Final Cover." *Journal of Geotechnical and Geoenvironmental Engineering*, 133(7), 814–827.
- Brachman, R. W. I., Rentz, A., Rowe, R. K., and Take, W. A. (2014). "Classification and quantification of downslope erosion from a geosynthetic clay liner (GCL) when covered only by a black geomembrane." *Canadian Geotechnical Journal*, 52(4), 395–412.
- Bradshaw, S., Benson, C., and Scalia IV, J. (2013). "Hydration and Cation Exchange during Subgrade Hydration and Effect on Hydraulic Conductivity of Geosynthetic Clay Liners." *Journal of Geotechnical and Geoenvironmental Engineering*, 139(4), 526–538.
- Bradshaw, S. L., Asce, A. M., Benson, C. H., Asce, F., and Rauen, T. L. (2015). "Hydraulic Conductivity of Geosynthetic Clay Liners to Recirculated Municipal Solid Waste Leachates." *Journal of Geotechnical and Geoenvironmental Engineering*, 142(2).
- Bradshaw, S. L., and Benson, C. H. (2014). "Effect of Municipal Solid Waste Leachate on Hydraulic Conductivity and Exchange Complex of Geosynthetic Clay Liners." *Journal of Geotechnical and Geoenvironmental Engineering*, 140(4), 4013038.
- Eun, J., Tinjum, J., Benson, C., and Edil, T. (2017). "Volatile Organic Compound (VOC) Transport through a Composite Liner with Co-Extruded Geomembrane Containing Ethylene Vinyl-Alcohol (EVOH)." *Journal of Geotechnical and Geoenvironmental Engineering*, 143(6), 1960–1969.
- Foose, G., Benson, C., and Edil, T. (1999). "Equivalency of Composite Geosynthetic Clay Liners as a Barrier to Volatile Organic Compounds." *Geosynthetics 99*, Industrial Fabrics Association International, St. Paul, 321–334.
- James, A. N., Fullerton, D., and Drake, R. (1997). "FIELD PERFORMANCE OF GCL UNDER ION EXCHANGE CONDITIONS." *Journal of Geotechnical and Geoenvironmental Engineering*, 123(10), 897–901.
- Jo, H.-Y., Benson, C. H., and Edil, T. B. (2004). "Hydraulic Conductivity and Cation Exchange in Non-Prehydrated and Prehydrated Bentonite Permeated with Weak Inorganic Salt Solutions." *Clays and Clay Minerals*, Clays and Clay Minerals, 52(6), 661–679.
- Jo, H., Katsumi, T., Benson, C. H., and Edil, T. B. (2001). "Hydraulic Conductivity and Swelling of Nonprehydrated GCLs Permeated with Single-Species Salt Solutions." *Journal of Geotechnical & Geoenvironmental Engineering*, 127(7), 557–567.
- Jo, H. Y., Benson, C. H., Shackelford, C. D., Lee, J.-M., and Edil, T. B. (2005). "Long-Term Hydraulic Conductivity of a Geosynthetic Clay Liner Permeated with Inorganic Salt Solutions." *Journal of Geotechnical and Geoenvironmental Engineering*, 131(4), 405–417.
- Koerner, R. (1990). *Designing With Geosynthetics*. (J. Scordato, ed.), Prentice-Hall Inc.,

Englewood Cliffs.

- Kolstad, D., Benson, C., and Edil, T. (2004a). "Hydraulic conductivity and swell of nonprehydrated geosynthetic clay liners permeated with multispecies inorganic solutions." *Journal of Geotechnical and Geoenvironmental Engineering*, 130(12), 1236–1249.
- Kolstad, D., Benson, C., Edil, T., and Jo, H. (2004b). "Hydraulic conductivity of a dense prehydrated GCL permeated with aggressive inorganic solutions." *Geosynthetics International*, 11(3), 233–241.
- Lake, C. B., and Rowe, R. K. (2005). "A comparative assessment of volatile organic compound (VOC) sorption to various types of potential GCL bentonites." *Geotextiles and Geomembranes*, 23(4), 323–347.
- Lee, J.-M., and Shackelford, C. D. (2005). "Concentration Dependency of the Prehydration Effect for a Geosynthetic Clay Liner." *Soils and Foundations*, Soils and Foundations, 45(4), 27–41.
- Lin, L., and Benson, C. H. (2000). "EFFECT OF WET-DRY CYCLING ON SWELLING AND HYDRAULIC CONDUCTIVITY OF GCLS." *Journal of Geotechnical & Geoenvironmental Engineering*, (January), 40–49.
- Luckham, P. F., and Rossi, S. (1999). "The colloidal and rheological properties of bentonite suspensions." *Advances in Colloid and Interface Science*, 82(1–3), 43–92.
- Meer, S. R., and Benson, C. H. (2007). "Hydraulic Conductivity of Geosynthetic Clay Liners Exhumed from Landfill Final Covers." *Journal of Geotechnical and Geoenvironmental Engineering*, 133(5), 550–563.
- Mitchell, J. K. (1993). *Fundamentals of Soil Behavior*. John Wiley & Sons, Inc., New York.
- Moore, D., and Reynolds, R. (1989). *X-Ray Diffraction and the Identification and Analysis of Clay Minerals*. Oxford University Press.
- Morris, G. E., and Zbik, M. S. (2009). "Smectite suspension structural behaviour." *International Journal of Mineral Processing*, 93(1), 20–25.
- Peel, M. C., Finlayson, B. L., and McMahon, T. A. (2007). "Updated world map of the Köppen-Geiger climate classification." *Hydrology and Earth System Sciences*, 11(5), 1633–1644.
- Petrov, R. J., and Rowe, R. K. (1997). "Geosynthetic clay liner (GCL) - chemical compatibility by hydraulic conductivity testing and factors impacting its performance." *Canadian Geotechnical Journal*, 34(6), 863–885.
- Petrov, R. J., Rowe, R. K., and Quigley, R. M. (1997a). "Comparison of Laboratory-Measured GCL Hydraulic Conductivity Based on Three Permeameter Types." *Geotechnical Testing Journal*, 20(1), 49–62.
- Petrov, R. J., Rowe, R. K., and Quigley, R. M. (1997b). "Selected Factors Influencing GCL Hydraulic Conductivity." *Journal of Geotechnical and Geoenvironmental Engineering*, 123(8), 683–695.
- Rao, S. M., Thyagaraj, T., and Raghuvver Rao, P. (2013). "Crystalline and Osmotic Swelling of an Expansive Clay Inundated with Sodium Chloride Solutions." *Geotechnical and Geological Engineering*, 31(4), 1399–1404.
- Rowe, R. K. (2012). "Short- and long-term leakage through composite liners." *Canadian Geotechnical Journal*, 49(2), 141–169.
- Rowe, R. K., Brachman, R. W. I., Take, W. A., Rentz, A., and Ashe, L. E. (2016). "Field and laboratory observations of down-slope bentonite migration in exposed composite liners." *Geotextiles and Geomembranes*, Elsevier Ltd, 44(5), 686–706.
- Rowe, R. K., Mukunoki, T., and Sangam, H. P. (2005). "BTEX diffusion and sorption for a geosynthetic clay liner at two temperatures." *Journal of Geotechnical and Geoenvironmental Engineering*, 131(10), 1211–1221.
- Rowe, R. K., Sangam, H. P., and Lake, C. B. (2003). "Evaluation of an HDPE geomembrane after 14 years as a leachate lagoon liner." *Canadian Geotechnical Journal*, 40(3), 536–550.
- Rowe, R. K., Take, W. A., Brachman, R. W. I., and Rentz, A. (2014). "Field observations of

- moisture migration on GCLs in exposed liners." *10th International Conference on Geosynthetics, ICG 2014*, (May 2010).
- Ruhl, J. L., and Daniel, D. E. (1997). "Geosynthetic Clay Liners Permeated with Chemical Solutions and Leachates." *Journal of Geotechnical and Geoenvironmental Engineering*, 123(4), 369–381.
- Scalia, J., and Benson, C. H. (2010a). "Effect of Permeant Water on the Hydraulic Conductivity of Exhumed GCLs." *Geotechnical Testing Journal*, 33(3), 1–11.
- Scalia, J., and Benson, C. H. (2010b). "Preferential flow in geosynthetic clay liners exhumed from final covers with composite barriers." *Canadian Geotechnical Journal*, 47(10), 1101–1111.
- Scalia, J., and Benson, C. H. (2011). "Hydraulic Conductivity of Geosynthetic Clay Liners Exhumed from Landfill Final Covers with Composite Barriers." *Journal of Geotechnical and Geoenvironmental Engineering*, 137(1), 1–13.
- Scalia, J., and Benson, C. H. (2016). "Polymer Fouling and Hydraulic Conductivity of Mixtures of Sodium Bentonite and a Bentonite-Polymer Composite." *Journal of Geotechnical and Geoenvironmental Engineering*, 143(4).
- Scalia, J., Benson, C. H., Albright, W. H., Smith, B. S., and Wang, X. (2017). "Properties of Barrier Components in a Composite Cover after 14 Years of Service and Differential Settlement." 143(9), 1–11.
- Scalia, J., Benson, C. H., Bohnhoff, G. L., Edil, T. B., and Shackelford, C. D. (2014). "Long-Term Hydraulic Conductivity of a Bentonite-Polymer Composite Permeated with Aggressive Inorganic Solutions." *Journal of Geotechnical and Geoenvironmental Engineering*, 140(3), 4013025.
- Schenning, J. a. (2004). "Hydraulic Performance of Polymer Modified Bentonite." University of South Florida.
- Shackelford, C. D., Benson, C. H., Katsumi, T., Edil, T. B., and Lin, L. (2000). "Evaluating the hydraulic conductivity of GCLs permeated with non-standard liquids." *Geotextiles and Geomembranes*, 18(2–4), 133–161.
- Shackelford, C. D., Sevick, G. W., and Eykholt, G. R. (2010). "Hydraulic conductivity of geosynthetic clay liners to tailings impoundment solutions." *Geotextiles and Geomembranes*, Elsevier Ltd, 28(2), 149–162.
- Take, W. A., Brachman, R. W. I., and Rowe, R. K. (2015). "Observations of bentonite erosion from solar-driven moisture migration in GCLs covered only by a black geomembrane." *Geosynthetics International*, 22(1), 78–92.
- Tian, K. (2015). "Long-Term Performance of Geosynthetic Liner Materials in Low-Level Radioactive Waste Disposal Facilities." University of Wisconsin-Madison.
- Tian, K., Benson, C. H., and Likos, W. J. (2017). "Effect of an anion ratio on the hydraulic conductivity of a bentonite-polymer geosynthetic clay liner." *Geotechnical Special Publication*, (GSP 276), 180–190.
- Trauger, R., and Darlington, J. (2000). "Next Generation Geosynthetic Clay Liners for Improved Durability and Performance." *Geosynthetic Research Institute Conference*, Las Vegas, 255–267.
- Vasko, S., young Jo, H., and Katsumi, T. (2001). "Hydraulic conductivity of partially prehydrated geosynthetic clay liners permeated with aqueous calcium chloride solutions." (Di), 685–699.
- Wagner, J. F., and Schnatmeyer, C. (2002). "Test field study of different cover sealing systems for industrial dumps and polluted sites." *Applied Clay Science*, 21(1–2), 99–116.